

# Materials and Systems for Organic Redox Flow Batteries: Status and Challenges

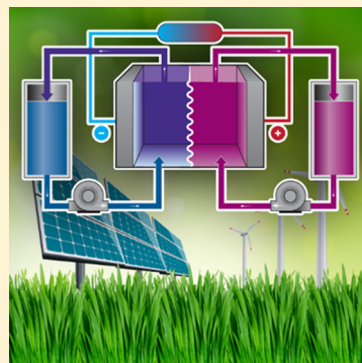
Xiaoliang Wei,<sup>\*,†,‡,§,ID</sup> Wenxiao Pan,<sup>§</sup> Wentao Duan,<sup>†,‡</sup> Aaron Hollas,<sup>‡</sup> Zheng Yang,<sup>†,‡</sup> Bin Li,<sup>‡</sup> Zimin Nie,<sup>‡</sup> Jun Liu,<sup>†,‡,§,ID</sup> David Reed,<sup>‡</sup> Wei Wang,<sup>‡,§,ID</sup> and Vincent Sprengle<sup>‡</sup>

<sup>†</sup>Joint Center for Energy Storage Research (JCESR), Argonne, Illinois 60439, United States

<sup>‡</sup>Energy & Environment Directorate, Pacific Northwest National Laboratory, 902 Battelle Boulevard, Richland, Washington 99354, United States

<sup>§</sup>Department of Mechanical Engineering, University of Wisconsin—Madison, 1513 University Avenue, Madison, Wisconsin 53706, United States

**ABSTRACT:** Redox flow batteries (RFBs) are propitious stationary energy storage technologies with exceptional scalability and flexibility to improve the stability, efficiency, and sustainability of our power grid. The redox-active materials are the key component for RFBs with which to achieve high energy density and good cyclability. Traditional inorganic-based materials encounter critical technical and economic limitations such as low solubility, inferior electrochemical activity, and high cost. Redox-active organic materials (ROMs) are promising alternative “green” candidates to push the boundaries of energy storage because of the significant advantages of molecular diversity, structural tailorability, and natural abundance. Here, the recent development of a variety of ROMs and associated battery designs in both aqueous and nonaqueous electrolytes are reviewed. The critical challenges and potential research opportunities for developing practically relevant organic flow batteries are discussed.



Electricity is central to the prosperity of our society. With the ever-growing global population, the demand for electricity is projected to increase from 21.6 trillion kWh in 2012 to 36.5 trillion kWh in 2040.<sup>1</sup> Concerns of limited resources, CO<sub>2</sub> emissions, and energy security have catalyzed a rapid transition from carbon-intensive fossil fuels to clean, abundant renewable energies. Solar and wind are the world’s fastest-growing energy sources for electricity production, with an average increase by 6.3% per year.<sup>1</sup> However, renewable energies are highly intermittent; the peak times of electricity generation and demand are often mismatched. It is estimated that the grid stability and service quality will be adversely affected when the renewable integration level reaches beyond 20%.<sup>2</sup> However, our current power infrastructure lacks sufficient measures to handle the electricity generation-demand discrepancies. The traditional way relies on redundant, under-utilized grid assets but is insufficient to cope with the more dynamic load in the future that will accompany higher renewable deployments. Addressing these challenges necessitates introduction of electrical energy storage systems to provide effective peak/off-peak managements and improve grid reliability through offering a time dimension. Given the large scale of stored energy, the most important requirements for grid storage technologies include cost-effectiveness, operational reliability, and safety. In this regard, electrochemical energy storage or rechargeable batteries have gained significant momentum among the many storage technologies; they also cover a

broad range of storage time and capacity to meet different grid applications (Figure 1a).<sup>3–6</sup> From the beginning of this decade until 2016, the number of worldwide electrochemical storage projects has grown from 58 to 692, with the rated power capacity from 0.17 to 1.64 GW (Figure 1b).<sup>7</sup> This ~10× increase reflects the heightened social awareness of the importance of electrochemical storage during the rapid evolution of our energy landscape.

**Redox Flow Battery.** Currently, lithium ion batteries (LIBs) dominate the global electrochemical storage market,<sup>8</sup> primarily because of their high energy densities and rapidly falling battery pack costs (state-of-the-art ~\$310 kWh<sup>-1</sup> with an annual decline rate of 8%).<sup>9,10</sup> However, key concerns about LIBs include irreversible aging due to phase transformations even when not in use and fire hazards due to the use of flammable organic electrolytes. Redox flow batteries (RFBs) have great potential to overcome these drawbacks. The energy-bearing redox-active materials are dissolved in liquid electrolytes stored in external reservoirs, as shown in Figure 2. Energy conversion occurs when the electrolytes are pumped to pass through porous electrodes. The electrodes serve to provide active sites for charge transfer without participating in electrochemical reactions. This unique battery design decouples the stored

Received: July 23, 2017

Accepted: August 25, 2017

Published: August 25, 2017

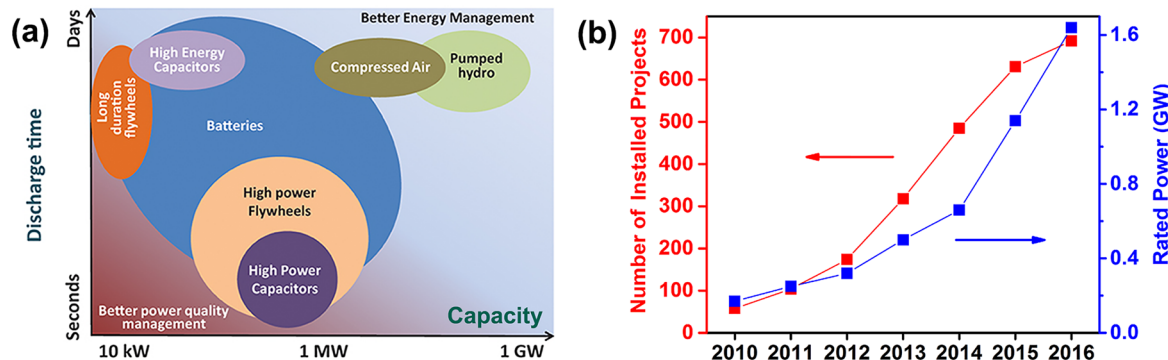


Figure 1. (a) Approximate representation of the discharge time and power capacity characteristics of storage technologies (reproduced with permission from Frontiers);<sup>6</sup> (b) global installation of electrochemical storage projects in the past 7 years.<sup>7</sup>

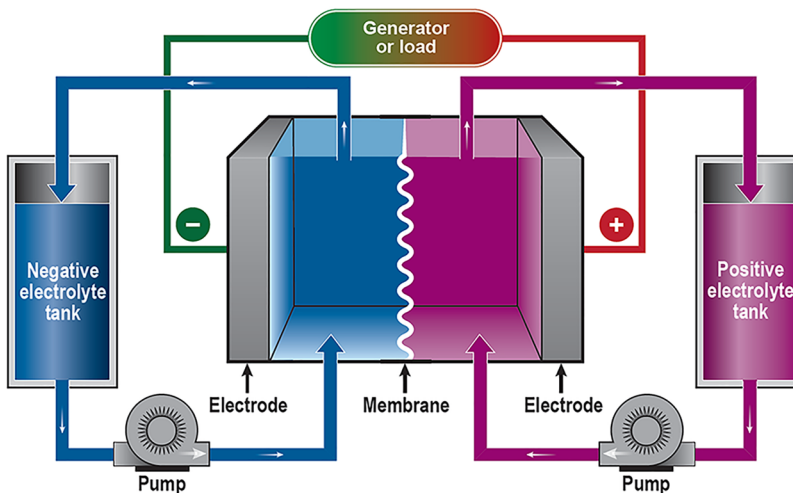


Figure 2. Schematic view of a RFB system.

energy and power, with the former determined by the electrolyte volume and the latter by the cell size. This feature enables independent scaling of energy and power, leading to significant advantages such as excellent scalability, modular manufacturing, flexible design, long life, active thermal management, and safety. Therefore, RFBs are widely recognized to be suitable for dispatchable, large-scale storage applications and have recently attracted substantial interest from academia, industry, utility, and government.

The redox-active materials are critically important for RFB systems because their properties determine the cycling performance (Figure 3a). For example, the solubility, redox potential, chemical stability, and cost of redox-active materials directly impact the energy density, cell voltage, cycle life, and cost intensity of a RFB system, respectively. Traditional RFBs are based on inorganic materials with an emphasis on metal species, such as all-vanadium (VRB),<sup>11,12</sup> iron/vanadium (IVB),<sup>13,14</sup> iron/chromium (ICB),<sup>15</sup> polysulfide/bromine (PSB),<sup>16</sup> zinc/bromine (ZBB),<sup>17</sup> zinc/polyiodide (ZIB),<sup>18</sup> zinc/cerium (Zn/Ce),<sup>19</sup> soluble lead-acid (SLFB),<sup>20</sup> hydrogen/bromine ( $H_2/Br_2$ ),<sup>21</sup> polysulfide/ferricyanide,<sup>22</sup> all-iron,<sup>23,24</sup> and so on. Several excellent reviews have introduced the historic advancements and provided comprehensive assessments of these RFBs.<sup>25–33</sup> Table 1 summarizes important materials properties, performance parameters, and key drawbacks of these systems, as well as organic-based systems for comparison. So far, the most promising system is the VRB that uses four different oxidation states of

the same element leading to minimal electrolyte cross-contamination and great long-term cyclability (>1000 stable cycles).<sup>34</sup> However, the system costs of VRBs ( $\$320 \text{ kWh}^{-1}$ , Figure 3b) are still substantially higher than the U.S. Department of Energy (DOE)'s cost target of  $\$100 \text{ kWh}^{-1}$ , with redox-active material comprising a major portion of the cost.<sup>35</sup> The key technical barrier that still limits the widespread market penetration of RFB technologies is the generally lower energy densities ( $<50 \text{ Wh L}^{-1}$ ) for most RFB systems compared to their LIB competitors ( $>200 \text{ Wh L}^{-1}$ ), as shown in Figure 3c. Only a few RFB chemistries such as zinc-based systems have energy densities of  $>50 \text{ Wh L}^{-1}$ , but other concurrent drawbacks limit their practical applications, including dendrite growth on metal anodes, irreversible materials crossover, gas evolutions, and/or slow electrochemical kinetics (see Table 1).

To overcome these limitations, strategies for improving the energy density of RFBs capitalize on developing new RFB designs and electrolytes to increase the cell voltage and effective concentration of redox-active materials. Novel RFB designs have been studied, such as nonaqueous RFBs,<sup>53,54</sup> hybrid Li/Na metal RFBs,<sup>55</sup> and flowable electrodes.<sup>48,56</sup> The primary motivation for pursuing nonaqueous RFBs is to harvest higher cell voltages ( $>2 \text{ V}$ ) and expand the library of material candidates made viable by the wide electrochemical windows (2–6.5 V). Hybrid Li/Na RFBs take advantage of the low redox potentials of  $Li/Li^+$  or  $Na/Na^+$  couples to obtain high cell voltages ( $>3 \text{ V}$ ). The anolyte typically contains lithium or sodium salts

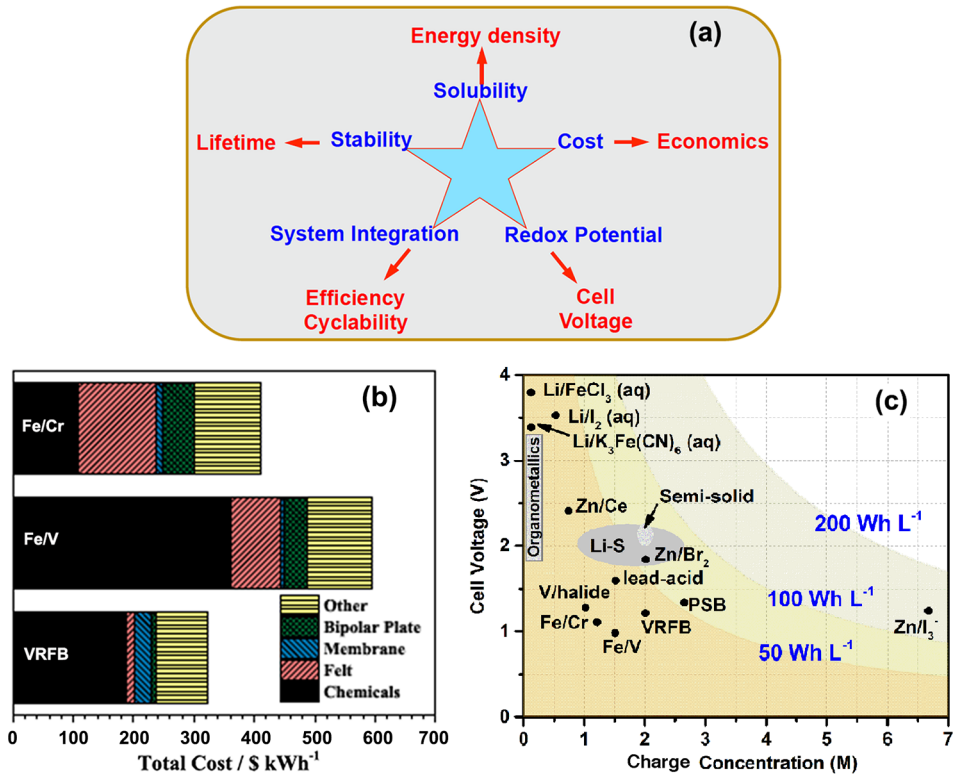


**Figure 3.** (a) Relationship between redox-active materials properties and RFB performance metrics; (b) cost breakdown of several RFBs at 1 MW/4 MWh scale (Reproduced with permission from Elsevier);<sup>35</sup> (c) approximate representation of the cell voltage, charge concentration (i.e., number of transferred electrons multiplied by redox material concentration), and energy density of various RFBs.

**Table 1. Important Parameters in Terms of Demonstrated Concentrations of Redox-Active Materials, Cell Voltage, Stability, System Integration, Cost, and Key Drawbacks of Major RFB Systems**

RFB systems	demonstrated charge concentration (M)	cell voltage (V)	stability	system integration	key drawbacks	element prices (\$ per 0.1 kg) <sup>36</sup>
VRB	3 <sup>37</sup>	1.25	>1000 stable cycles <sup>38</sup> –5–50 °C range	84% @ 100 mA cm <sup>-2</sup> <sup>39</sup>	high chemical cost	V: 2.7 <sup>a</sup>
ICB	1.25	1.18	30–100 cycles, 0.3%/cycle fading <sup>40</sup>	78% @ 65 °C and 120 mA cm <sup>-2</sup> <sup>40</sup>	slow kinetics; H <sub>2</sub> evolution	Fe: 0.02 <sup>a</sup>
IVB	1.5	1.02	>100 stable cycles 0–50 °C range <sup>13</sup>	82% @ 50 mA cm <sup>-2</sup>	high chemical cost	Cr: 0.28 <sup>a</sup>
PSB	2.6	~1.5	50 cycles <sup>41</sup>	77% @ 50 mA cm <sup>-2</sup>	Br <sub>2</sub> crossover; S precipitation; slow kinetics	Br: 0.15 <sup>a</sup> Zn: 0.18 <sup>a</sup>
ZBB	4	1.76	300 stable cycles <sup>42</sup>	81% @ 80 mA cm <sup>-2</sup>	zinc dendrite; low utilization	Pb: 0.02 <sup>a</sup>
ZIB	6.67	1.30	50 stable cycles –20–50 °C range <sup>18</sup>	75% @ 20 mA cm <sup>-2</sup> <sup>43</sup>	zinc dendrite; high cost	Ce: 1.2 <sup>a</sup> Cu: 0.66 <sup>a</sup>
Zn/Ce	0.8 <sup>19</sup>	2.4	~50 cycles <sup>19</sup>	63% @ 50 mA cm <sup>-2</sup> <sup>19</sup>	gas evolution	S: 0.01 <sup>a</sup>
SLFB	1 <sup>44</sup>	1.59	2000 cycles <sup>20</sup> or 100 stable cycles <sup>44</sup>	79% @ 20 mA cm <sup>-2</sup> <sup>20</sup>	Pb dendrite; PbO <sub>2</sub> polymorph	Cl: 0.15 <sup>b</sup>
H <sub>2</sub> /Br <sub>2</sub>	1 <sup>21</sup>	1.09	100 stable cycles <sup>45</sup>	65% @ 400 mA cm <sup>-2</sup> <sup>45</sup>	costly Pt catalyst; Br <sub>2</sub> crossover	I: 8.3 <sup>b</sup>
Li/aqueous	0.5 <sup>46</sup>	~3.5	20 stable cycles <sup>46</sup>	~90% @ 2.5 mA cm <sup>-2</sup> <sup>46</sup>	costly membrane; fire hazard; limited charge rate	H: 12 <sup>b</sup>
semisolid	>10	>2	100 cycles <sup>47</sup>	~75% @ C/8 <sup>48</sup>	suspension stability; high viscosity shunt; current loss	
organic RFB	up to 4 <sup>49</sup>	up to 4 <sup>50</sup>	up to 700 stable cycles <sup>49</sup>	50–60% @ 500 mA cm <sup>-2</sup> <sup>51</sup>	still in the infancy stage	as low as \$1 per kg <sup>52</sup>

<sup>a</sup>In bulk form. <sup>b</sup>In pure form.

dissolved in organic solvents, while the catholytes can use aqueous<sup>46,57,58</sup> or nonaqueous<sup>59–62</sup> electrolytes. Instead of static carbon electrodes, RFBs with flowable electrodes are based on percolating nanoscale conductor networks cosuspended with LIB

electrode particles in battery electrolytes. These semisolid RFBs are a synergy between LIBs and RFBs that enables high energy density (>10 M electron concentrations) while still maintaining RFB characteristics, although the flowability may be compromised

at high material loadings. Other types of studied redox materials with competitive solubilities include metal coordination complexes (MCCs),<sup>63</sup> polyoxometalates,<sup>64</sup> and metal ionic liquids.<sup>65</sup> Notably, MCCs based on redox noninnocent ligands can enable multiple electron transfers to achieve increased energy density.<sup>66,67</sup>

Redox-active organic materials (ROMs) have recently attracted intense research attention as alternative energy materials for

**Redox-active organic materials (ROMs) have recently attracted intense research attention as alternative energy materials for achieving high-energy-density, cost-effective RFBs.**

achieving high-energy-density, cost-effective RFBs. Compared to insoluble organic electrode materials used for metal ion batteries,<sup>68–70</sup> the development of ROM-based RFBs pursues an opposite direction in terms of high solubility. The use of ROMs provides tremendous flexibility, with a diverse range of molecular structures and corresponding electrochemical mechanisms as well as synthetic tunability that can adjust the redox potential, solubility, and ionic charge, all of which enable significant leeway in overall RFB design. In addition, many ROMs exist abundantly in nature, making them “green”, safe, inexpensive materials. ROM families being investigated for RFBs include metallocenes, dialkoxybenzenes, carbonyls (including quinones), nitroxide radicals, and heterocyclic aromatics, as depicted in Figure 4 (methyl viologen (MV) is shown as an example for

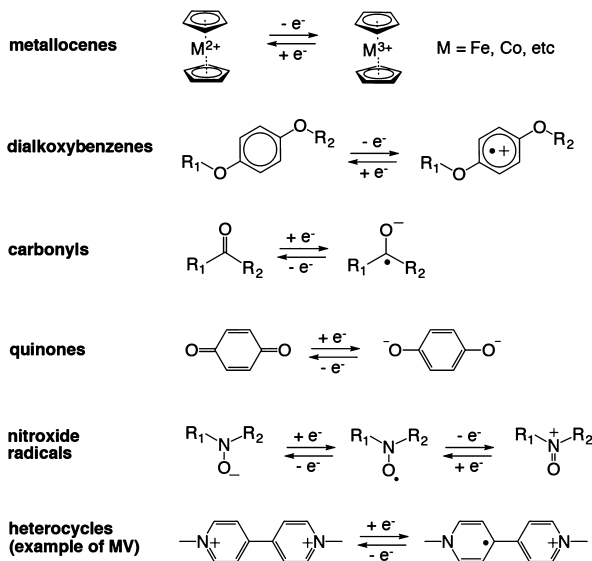


Figure 4. Electrochemical reactions of ROMs used in RFBs.

heterocyclic aromatics); also shown are their electrochemical reactions. Due to the wide distribution of redox potentials, these materials have been used as either anolyte or catholyte materials in nonaqueous and aqueous RFBs. Here, metallocenes are categorized as ROMs because of their facile tailorability, although they are in fact organometallic compounds. Although still in the infancy developmental stage, a few ROM-based RFBs have generated exceeding materials and performance metrics compared to traditional inorganic-based systems, as summarized in Table 1 and detailed in the following sections.<sup>71–73</sup>

Despite the impressive progress, practical scale-up installations of organic RFBs have yet to become reality because of the existing technical and financial hurdles. Compared with the benchmark VRB system, only very few ROMs possess a combination of compelling properties in terms of solubility, redox potential, cost, and stability, which makes it even more challenging to couple two such ROMs into RFB chemistry of practical significance. To further advance the organic RFB technology, it is essential to extract the developmental pipeline from prior ROM design and prototyping efforts. For this purpose, this Review highlights the major accomplishments in recent ROM research and conveys the acquired fundamental understandings of ROM structure–property relationships and failure mechanisms. This knowledge has contributed to rationalize the design principles and protocols to guide the R&D of new ROMs with improved solubility and stability. Following the detailed introductions of each ROM family in both aqueous and nonaqueous RFBs, the emerging RFB material/system designs and the role of computational modeling in ROM discovery are presented. Finally, key challenges and research perspectives are briefly discussed.

**ROM Families for RFBs.** *Metallocenes.* Metallocenes are a family of sandwich compounds consisting of two aromatic cyclopentadienyl anions ( $Cp$ ,  $C_5H_5^-$ ) bound to a metal ion center that undergoes  $1 e^-$  transfer. The most studied metallocene in RFBs is ferrocene (Fc), garnering attention as a promising catholyte because of its favorable redox potential ( $\sim 3.44$  V vs Li/Li $^+$ ),<sup>74</sup> high stability, and reversible electrochemistry in both aqueous and nonaqueous systems. Figure 5a illustrates reported Fc derivatives, with Fc,<sup>62,75</sup> Fc-TFSI,<sup>61,76</sup> Fc-Br,<sup>77</sup> and DMFc<sup>78</sup> investigated in nonaqueous RFBs while FcNCl<sup>49</sup> and DTMAP-Fc<sup>79</sup> have been used in aqueous RFBs. Typically, structural tailoring via incorporating polar groups is necessary to facilitate dissolution of the nearly insoluble pristine Fc to relevant levels, for example, 1.7 M for Fc-TFSI in carbonates,<sup>61</sup> 4.0 M for FcNCl in water,<sup>49</sup> and 1.9 M for DTMAP-Fc in water.<sup>79</sup> Nuclear magnetic resonance (NMR) studies and density functional theory (DFT) calculations demonstrated increased solvation interactions with solvent molecules at the polar motifs, such as the quaternary ammonium pendants in Fc-TFSI.<sup>61,80–82</sup> Introduction of electron-withdrawing quaternary ammonium groups to the cyclopentadienyl ring also caused positive shifts in redox potential of Fc, leading to higher cell voltages.<sup>49,61</sup> Interestingly, by reducing molecular symmetry, alkyl substituents can greatly decrease the melting point and increase the solubility of Fc in aprotic solvents; for example, DMFc could dissolve up to 3 M in the presence of 3 M LiClO<sub>4</sub> in carbonate.<sup>78</sup>

In nonaqueous RFBs, Fc derivatives have been extensively evaluated in hybrid Li/Fc systems (Figure 5b) to harvest high energy densities. The cell voltages ranged between 3.1 and 3.7 V vs Li/Li $^+$  depending on Fc structures and supporting electrolytes.<sup>62,83,84</sup> Typically, these Li/Fc flow cells at low concentrations of Fc derivatives (i.e., 0.05–0.1 M) produced high Coulombic efficiency (CE) of >99% and good cycling stability with high capacity retention for several hundreds of cycles, primarily because of the high stability and reversibility of Fc species. Another important contribution to such cyclability was from the stabilization of solid electrolyte interphase (SEI) layers by electrolyte additives, such as fluoroethylene carbonate (FEC) or LiNO<sub>3</sub>, which led to low self-discharge and stable Li deposition/dissolution reactions. In addition, the rapid electrochemical kinetics of Fc also led to high rate performance in

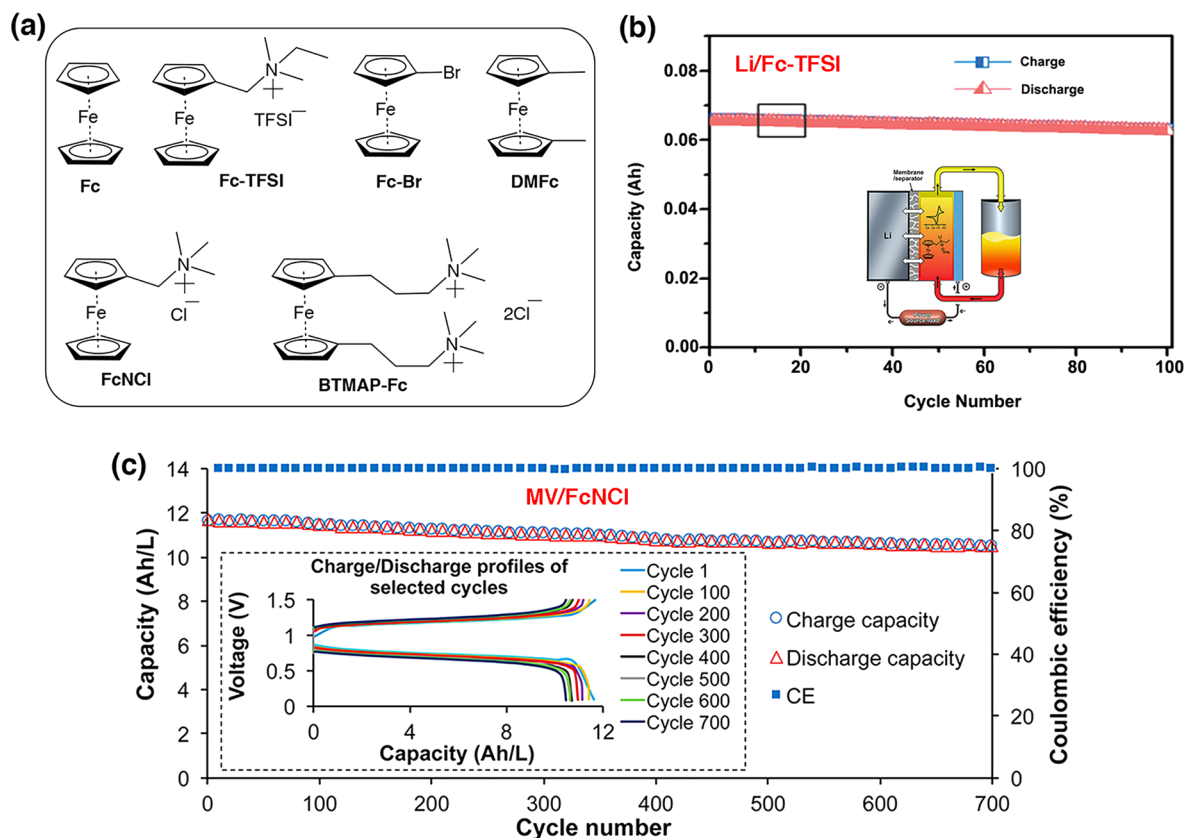


**Figure 5.** (a) Structures of reported Fc derivatives; (b) schematic view (inset) and cycling capacities of a nonaqueous Li/Fc-TFSI flow cell at 0.1 M Fc-TFSI (Adapted with permission from Wiley);<sup>61</sup> (c) cycling capacity and voltage curves of an aqueous MV/FcNCl RFB (Reproduced with permission from the American Chemical Society).<sup>49</sup>

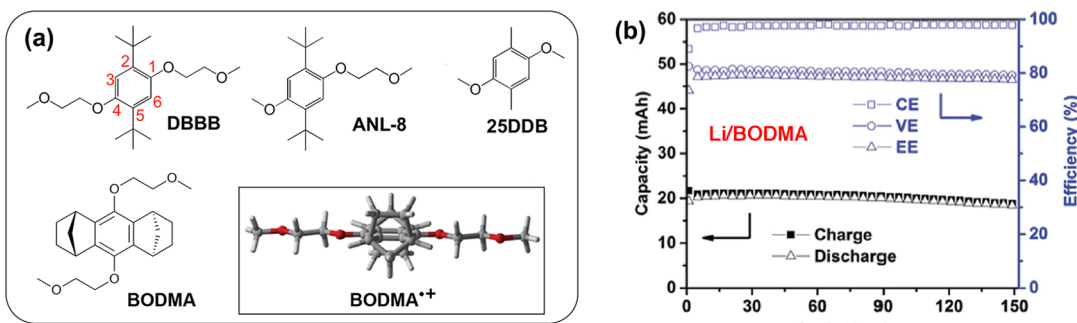


**Figure 6.** (a) Structures of dialkoxybenzene derivatives (inset: calculated lowest-energy molecular configuration of BODMA<sup>++</sup>); (b) cycling performance of the 0.1 M Li/BODMA flow cell with stable capacities (Reproduced with permission from Wiley).<sup>50</sup>

Li/Fc cells; for example, a material utilization of 86% could be achieved at a charge rate as high as 60C.<sup>75</sup> When higher concentrations of Fc species were used, more effective Li anode protection was needed to enable decent cyclability. Wang et al. demonstrated that a hybrid anode consisting of directly stacked Li and graphite felt strips could shift Li deposition/dissolution reactions to Li<sup>+</sup>-ion intercalation reactions, which reduced Li metal involvement and offered improved Li protection, while still keeping the same redox potential as Li/Li<sup>+</sup>.<sup>61</sup> A Li-graphite/Fc-TFSI flow cell at 0.8 M Fc-TFSI delivered stable cycling for ~20 cycles with a high volumetric energy density of 50 Wh L<sup>-1</sup>. However, despite these encouraging results, the Li anode still lacks sufficient protection to enable long-term stable RFB operations under battery-relevant conditions, which is also a general limitation for Li metal batteries.

Other than Li/Fc RFBs, nonaqueous all-metallocene RFBs were also developed. Yu et al. developed a nonaqueous all-metallocene RFB that achieved greatly increased cell voltage via rational solvent tuning.<sup>83</sup> Coupling an anolyte of cobaltocene in 1,3-dioxolane (DOL) with a catholyte of Fc in N,N-dimethylformamide (DMF) yielded a higher cell voltage of 1.8 V, compared to 1.3 V when using the same solvent. Although relatively stable cycling for 30 cycles was demonstrated, this RFB required the use of expensive LISICON-type ceramic separators to block crossover of solvents and metallocenes, which compromises the scalability of this system. Further material tailoring expanded the cell voltage to 2.1 V when the cobaltocene was decorated with 10 electron-donating methyl groups. Kim et al. also demonstrated that functionalizing metallocenes to bromoferrocene and

decamethylcobaltocene led to an expanded cell voltage of 2.0 V in acetonitrile.<sup>77</sup>

In aqueous RFBs, Fc derivatives have been paired with disubstituted viologen compounds in neutral electrolytes. Due to their cationic nature, anion exchange membranes were used in these RFBs to reduced materials crossover. Liu et al. demonstrated a MV/FcNCl RFB system that delivered 700 cycles of stable cycling with no detectable materials degradation or crossover (Figure 5c).<sup>49</sup> A similar system with differently tailored viologen and Fc species was developed by Aziz et al. that produced exceptional stability with 98.6% capacity retention over 250 cycles at ROM concentrations of 1.3 M.<sup>79</sup> Such performances are among the longest cyclability of ROM-based RFBs, primarily ascribed to the high stability of these electrochemical reactions. Although these flow cells were tested at redox concentrations lower than their solubility limits, the impressive results indicate that Fc derivatives are promising catholyte material candidates for practically feasible RFB systems. Further work should address the challenges associated with cell optimizations at high-concentration regimes.

**Dialkoxybenzenes.** 1,4-Dialkoxybenzenes are usually used as catholyte materials because of their high redox potentials of ~3.9 V vs Li/Li<sup>+</sup>. Dialkoxybenzenes form a water-unstable radical cation upon electrochemical oxidation; therefore, this class of ROM can only be used in nonaqueous RFBs. Derivatives typically bear oligo(ethylene glycol) ether side chains to increase their solubility in battery solvents (Figure 6a). To offer good stability for RFB applications, alkyl substituents at 2-, 3-, 5-, or 6-positions are required to provide steric hindrance against incoming nucleophilic attack, with the bulky *tert*-butyl group offering the best protection. The first reported dialkoxybenzene RFB coupled 2,5-di-*tert*-butyl-1,4-bis(2-methoxyethoxy)benzene (DBBB) with quinoxaline derivatives to form an all-organic RFB.<sup>85,86</sup>

To increase the solubility of DBBB (<0.4 M in carbonates), breaking the molecular symmetry was found to significantly

Compared with the benchmark VRB system, only very few ROMs possess a combination of compelling properties in terms of solubility, redox potential, cost, and stability, which makes it even more challenging to couple two such ROMs into RFB chemistry of practical significance. To further advance the organic RFB technology, it is essential to extract the developmental pipeline from prior ROM design and prototyping efforts.

decrease its melting point and afford a liquid derivative, ANL-8 (Figure 6a).<sup>87</sup> Because of its ready miscibility with battery solvents, ANL-8 is favored for RFB applications because the electrolyte will need no or a minimum amount of solvent to afford liquidity and achieve high energy density. ANL-8 has been evaluated in bulk electrolysis (BE) cells and also in several all-organic RFB systems that produced decent cyclability.<sup>88–90</sup> To improve the gravimetric charge density, a “molecular pruning” strategy was adopted to remove nonessential structural motifs from ANL-8.<sup>91,92</sup> This led to the development of 2SDDB (Figure 6a), the lightest organic radical cation that has the highest specific charge storage capacity reported so far (161 mAh g<sup>-1</sup>).

Despite these advantages, the radical cations of these analogues lack sufficient stability, as evidenced by the continuous capacity fading in corresponding Li/organic flow cells.<sup>92</sup> To overcome this limitation, a bicyclic substitution approach was used to develop the stable derivative, BODMA (Figure 6a).<sup>50</sup>

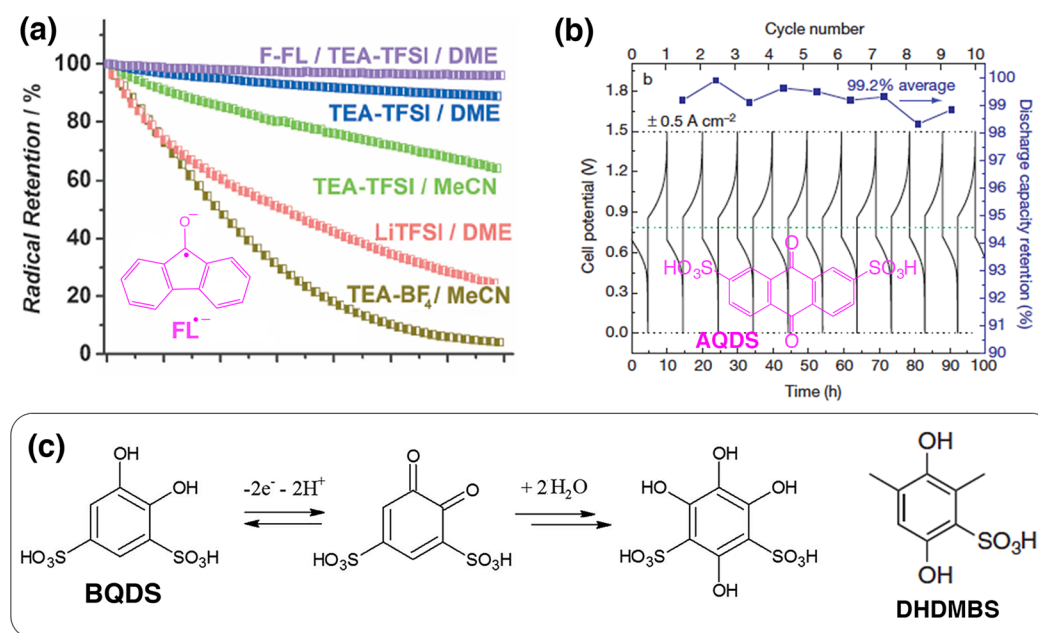
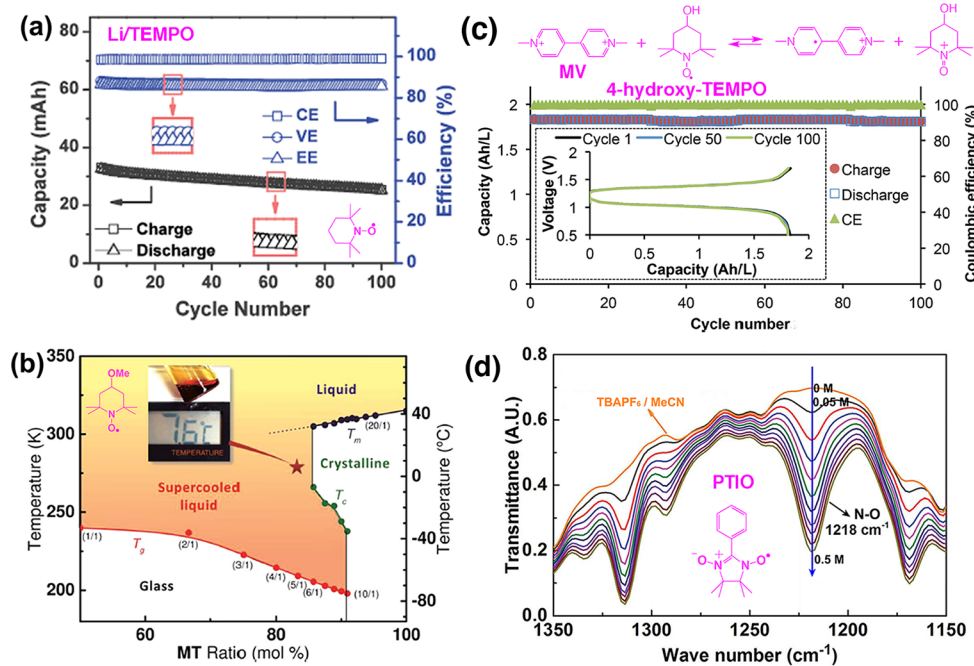


Figure 7. (a) Effects of supporting solvents and salts on the chemical stability of  $\text{FL}^{\bullet-}$  with the compositions of 0.1 M  $\text{FL}^{\bullet-}$  in 1 M salts (Adapted with permission from Wiley);<sup>88</sup> (b) voltage curves and CE of the aqueous AQDS/bromine RFB at  $0.5 \text{ A cm}^{-2}$  (Adapted with permission from Springer Nature);<sup>51</sup> (c) degradation of BQDS via a Michael addition pathway and the derived stable candidate DHDMBS (Adapted with permission from Electrochemical Society).<sup>93</sup>



**Figure 8.** (a) Cycling efficiencies and capacities of a Li/TEMPO flow cell at 0.1 M TEMPO (Adapted with permission from Wiley);<sup>102</sup> (b) phase diagram of the MT-LiTFSI solvate ionic liquids (Adapted with permission from Wiley);<sup>105</sup> (c) electrochemistry and 0.1 M flow cell performance of an aqueous RFB based on MV anolyte and 4-hydroxy-TEMPO catholyte (Adapted with permission from Wiley);<sup>52</sup> (d) Beer–Lambert dependence of the FTIR peaks on the PTIO concentration in the range of 1150–1350 cm<sup>−1</sup> (Adapted with permission from The Royal Society of Chemistry).<sup>106</sup>

The improved stability of BODMA<sup>•+</sup>, demonstrated by the 150 cycles of stable cycling of a Li/BODMA flow cell (Figure 6b), was argued to originate from a physical organic principle. The constrained conformation induced by the [2:2:1]heptane-like bicyclic substituents opens up the space for the alkoxy chains to freely rotate into the arene plane (Figure 6a inset), so that the lone pairs on O are better delocalized in the electron-deficient arene ring to acquire additional stability. Due to the hydrophobicity of the bicyclic rings, the solubility of BODMA is not high (0.15 M).<sup>50</sup> Further work to improve its solubility could proceed through incorporation of polar groups or engineering molecular asymmetry, as previously described.

**Carbonyl Compounds.** Carbonyl groups (C=O) undergo 1 e<sup>−</sup> transfer to form radical anions (•C—O<sup>−</sup>). To make carbonyls feasible for RFB applications, stabilization of the chemically reactive radical anions necessitates spin and charge delocalization. Wei et al. coupled a 9-fluorenone (FL) anolyte, where the spin and charge in FL<sup>•−</sup> were resonated onto the fused aromatic rings, with ANL-8 catholyte to obtain a nonaqueous all-organic RFB.<sup>88</sup> The supporting salts and solvents were demonstrated to significantly affect the chemical stability of FL<sup>•−</sup>, as evidenced by electron paramagnetic resonance (EPR) studies (Figure 7a). This behavior is associated with the side reaction pathways of FL<sup>•−</sup>. The FL<sup>•−</sup> could nucleophilically attack electron-deficient groups in electrolyte molecules, for example, —H and —C≡N in acetonitrile, C=O in carbonates, and BF<sub>4</sub><sup>−</sup> in salt, or undergo pinacol coupling to form FL–FL dimers. Use of relatively electron-neutral battery reagents such as 1,2-dimethoxyethane (DME) and tetraethylammonium bis(trifluoromethylsulfonyl)imide (TEA-TFSI) could mitigate these side reactions and yield more stable cycling. Similar phenomena were observed in a separate all-organic system based on N-methylphthalimide anolyte and ANL-8 catholyte.<sup>89</sup> These insights of degradation mechanisms can guide rational

electrolyte design and optimization for achieving stable organic RFBs.

Interestingly, with two conjugated carbonyl groups, quinones show greatly improved stability for 2e<sup>−</sup> processes, with the redox potentials also positively shifted due to the electron-withdrawing C=O groups. In nonaqueous electrolytes, the 2e<sup>−</sup> transfer is stepwise, forming the radical anion and then proceeding to the dianion. Wang et al. investigated a Li/organic RFB using structurally tailored anthraquinone as the catholyte material.<sup>94</sup> The stepwise reactions were clearly demonstrated by the two sets of redox peaks in cyclic voltammograms and the two plateaus in cell voltage curves.

On the contrary, in aqueous electrolytes, the 2e<sup>−</sup> processes of quinones (Brushett et al. claimed 1.5 e<sup>−</sup> instead<sup>95</sup>) occur in one step as a concerted proton coupled electron transfer (PCET) event. Aziz et al. demonstrated the first metal-free, ROM-based aqueous RFB based on the highly soluble anthraquinone disulfonic acid (AQDS) anolyte coupled with bromine catholyte in acidic electrolytes (Figure 7b).<sup>51</sup> This RFB delivered a remarkably high power density of 1 W cm<sup>−2</sup> at a state of charge (SOC) of 90%, reflecting the fast kinetics of both redox pairs.<sup>96</sup> However, the crossover of bromine species necessitates the use of excessive bromine catholyte to maintain stable cycling capacity. Further study indicated that the presence of electron-donating aryl hydroxyl groups could activate parasitic bromination side reactions with crossed-over bromine.<sup>97</sup> Later, Aziz et al. reported an alkaline RFB using 2,6-dihydroxyanthraquinone (DHAQ) anolyte coupled with ferrocyanide catholyte.<sup>98</sup> The DHAQ exploited the high pH to negatively shift its redox potential, leading to a high cell potential of 1.2 V. This RFB demonstrated relatively stable cycling with high cell efficiencies for 100 charge/discharge cycles.

Compared to anthraquinones, quinones without the two electron-donating benzo groups show much higher redox potentials.

Narayanan et al. demonstrated an all-quinone RFB using 1,2-benzoquinone-3,5-disulfonic acid (BQDS) anolyte and anthraquinone-2-sulfonic acid (AQS) catholyte.<sup>99</sup> Following a mechanistic study revealing BQDS degradation via a Michael addition pathway,<sup>100</sup> a stable derivative, 3,6-dihydroxy-2,4-dimethylbenzenesulfonic acid (DHDMBS), was developed with improved chemical stability that enabled longer cycling (Figure 7c).<sup>93</sup>

**Organic Nitroxide Radicals.** Nitroxide radicals contain an aminoxy group that is characterized by a two-center, three-electron (2c3e) N–O bond. The spin density is distributed on both N and O atoms by structural resonance, typically being slightly higher on O. Stable nitroxide radicals generally have alkyl or aryl substituents  $\alpha$  to N because a H atom at this position leads to spontaneous disproportionation side reactions. (2,2,6,6-Tetramethylpiperidin-1-yl)oxyl (TEMPO), with four methyl groups adjacent to the N–O bond offering steric protection, is one of the most persistent radicals. A variety of TEMPO derivatives have been evaluated in both aqueous and nonaqueous RFBs because of the stability and reversibility of the electrochemical reactions.

TEMPO has a high dipole moment of  $\sim 3.0 \text{ D}^{101}$  that affords a low melting point ( $36\text{--}38^\circ\text{C}$ ) and good solubility in polar organic solvents, for example, 5.2 M in a carbonate mixture.<sup>102</sup> This advantage, as well as its redox potential at  $\sim 3.5 \text{ V vs Li/Li}^+$ , makes TEMPO a highly promising catholyte material for nonaqueous RFBs. Wang et al. demonstrated Li–graphite/TEMPO flow cells that produced relatively good cycling stability over 100 cycles at low TEMPO concentrations (Figure 8a).<sup>102</sup> At 2.0 M TEMPO, although plagued with capacity fading, the flow cell delivered an impressive energy density of  $183 \text{ Wh L}^{-1}$  during charge and  $126 \text{ Wh L}^{-1}$  during discharge. Moreover, TEMPO-based nonaqueous all-organic RFBs, including TEMPO/N-methylphthalimide (1.6 V in acetonitrile)<sup>103</sup> and 4-oxo-TEMPO/(1S)-(+)-camphorquinone (2.1 V in PC),<sup>104</sup> have also been studied.

Interestingly, TEMPO species can form liquid-phase deep eutectic electrolytes (DEEs) with lithium salts without adding any solvents. Takechi et al. demonstrated that 4-methoxy-TEMPO (MT) forms DEEs (called “solvate ionic liquids” in this literature) with LiTFSI in the molar ratio range of 1:1 to 20:1.<sup>105</sup> The DEEs at specified compositions remained in the liquid phase over a broad temperature range even as low as  $-70^\circ\text{C}$  (Figure 8b). This was ascribed to the strong solvation interactions between MT and  $\text{Li}^+$  leading to formation of liquefied ionic couples between  $(\text{Li-MT})^+$  and  $\text{TFSI}^-$ . When directly used as the catholyte in a hybrid Li metal RFB, the DEE system resulted in a significantly high energy density of  $200 \text{ Wh L}^{-1}$ .

In aqueous RFBs, TEMPO needs to be functionalized with hydrophilic groups at the para position to make it water-soluble. Liu et al. demonstrated a 1.25 V aqueous RFB using highly soluble 4-hydroxy-TEMPO catholyte coupled with a heterocyclic MV anolyte (Figure 8c).<sup>52</sup> The inexpensiveness of these two compounds and the hydrocarbon membrane led this RFB to a capital cost of \$180 per kWh, significantly lower than \$320 per kWh for VRBs. This RFB produced stable cycling capacity for 100 cycles at 0.1 M redox materials but encountered continuous capacity fading at higher concentrations (e.g., 0.5 M). Schubert et al. developed alternative TEMPO species with trimethylammonium or sulfonate substituents at the para position, with the former derivative coupled with MV anolyte and the latter with a zinc anode, respectively; both RFB systems produced relatively stable cycling.<sup>107,108</sup>

Nitroxide radicals are capable of ambipolar electrochemical reactions to form the aminoxy anion when electrochemically reduced by  $1 \text{ e}^-$  and the oxoammonium cation when oxidized by  $1 \text{ e}^-$  (Figure 4). This feature makes nitroxide radicals potential candidates for symmetric RFBs that are based on a single ROM molecule. However, the aminoxy anion species of TEMPO is not stable in battery electrolytes. Wei et al. demonstrated a cyclable symmetric nonaqueous RFB using the more stable PTIO (Figure 8d).<sup>106,109</sup> The ambipolar reactions of PTIO occurred at the same N–O bond, and the reaction between  $\text{PTIO}^+$  and  $\text{PTIO}^-$  regenerated neutral PTIO. Ideally, use of PTIO in the symmetric RFB could recover the capacity loss if material crossover was the major cause. However, due to the instability of  $\text{PTIO}^-$ , the flow cells suffered from continuous capacity fading. Interestingly, the SOCs of the PTIO battery were accurately measured by FTIR that was cross-validated by EPR. On the basis of the N–O peak at  $1218 \text{ cm}^{-1}$ , FTIR successfully distinguished among the three redox states of PTIO, had negligible interference from the solvent and salt, and exhibited a Beer–Lambert dependence on the PTIO concentration (Figure 8d). This work is expected to inspire more insight into the underaddressed area of real-time SOC monitoring that aims for RFB operational safety. Similar to the PTIO chemistry, Carretero González et al. developed symmetric aqueous RFBs based on indigo carmine derivatives with tailored electrolytes greatly increasing the solubility, but no flow cell data were reported.<sup>110</sup> In a sense, the symmetric RFB design is similar to that of VRB and is expected to minimize irreversible material crossover and enable long-term cyclability.<sup>111</sup> The key challenge lies in how to achieve high solubilities and stabilities for all three redox states. This should be an important direction in developing practically viable RFBs.

**Heterocyclic Aromatics.** Heterocycles are cyclic compounds in which at least one carbon atom in the backbone ring is replaced by a heteroatom such as nitrogen, sulfur, oxygen, and so forth. Typically, these heteroatoms have a significant contribution to the frontier molecular orbitals of redox-active heterocycles. The aromatic structures offer good chemical stability necessary for RFB applications because of spin and charge delocalization. Heterocyclic aromatics exhibit a broad distribution of redox potentials and can be used as either anolyte or catholyte materials in nonaqueous and aqueous RFBs.

Brushett et al. studied quinoxaline anolytes to couple with DBBB catholyte in a nonaqueous all-organic RFB.<sup>85</sup> Quinoxalines exhibited high solubilities of up to 7 M in carbonate, stepwise  $2 \text{ e}^-$  transfer at  $\sim 2.6$  and  $\sim 2.9 \text{ V vs Li/Li}^+$ , and tunable stability via introduction of alkyl substituents. The RFB produced relatively stable capacity for 30 cycles, albeit with a low cell voltage of  $\sim 1.3 \text{ V}$  due to the relatively high redox potential of the quinoxaline. Such redox potentials even make quinoxalines fall within the water splitting window and be used for aqueous RFB applications.<sup>112</sup> Sanford et al. developed a series of low-potential *N*-alkylated pyridinium derivatives as anolyte materials for nonaqueous RFBs.<sup>113</sup> A physical organic approach was adopted to tune the substituents in the molecules to steer steric protection and achieve persistent charged radical species.<sup>114</sup> This study led to identification of the pyridinium analogue 17 (Figure 9a) that produced stable cycling in BE cells at 95% SOC for 200 cycles without detectable capacity loss. Wei et al. demonstrated a 2,1,3-benzothiadiazole (BzNSN) anolyte that was coupled with ANL-8 catholyte in nonaqueous electrolytes.<sup>90</sup> The low arene charge density offered good chemical stability for the radical anions to alleviate reactivity

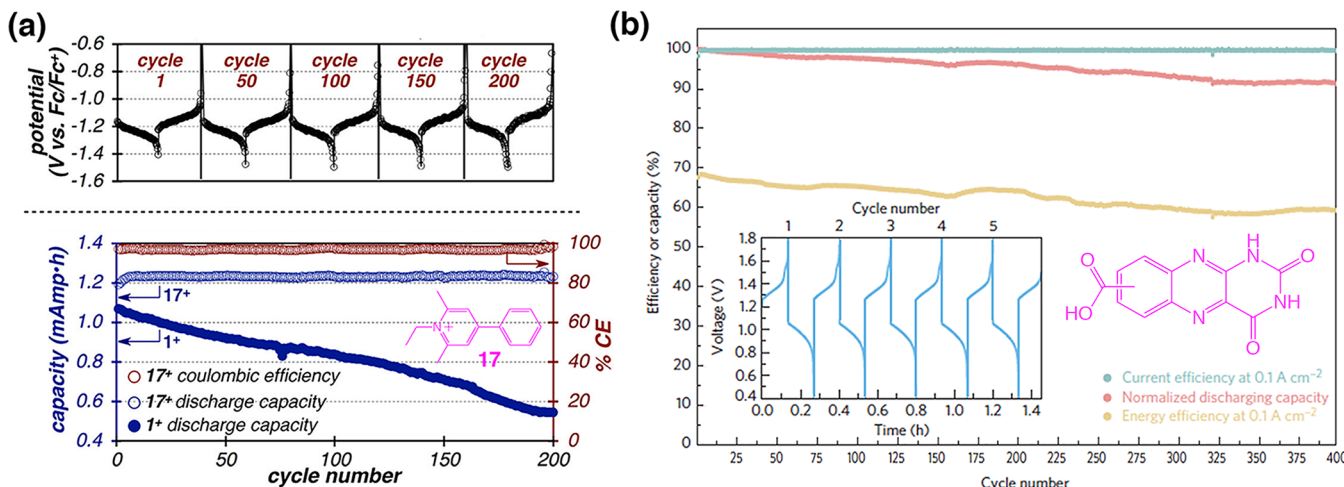


Figure 9. Cycling efficiencies, capacities, and/or voltage curves of heterocyclic aromatics-based RFBs: (a) nonaqueous BE cells of 10 mM pyridinium 17 (Adapted with permission from the American Chemical Society);<sup>114</sup> (b) an alkaline alloxazine/ferrocyanide RFB with 0.5 M alloxazine carboxylic acid at  $0.1 \text{ A cm}^{-2}$  (Adapted with permission from Springer Nature).<sup>117</sup>

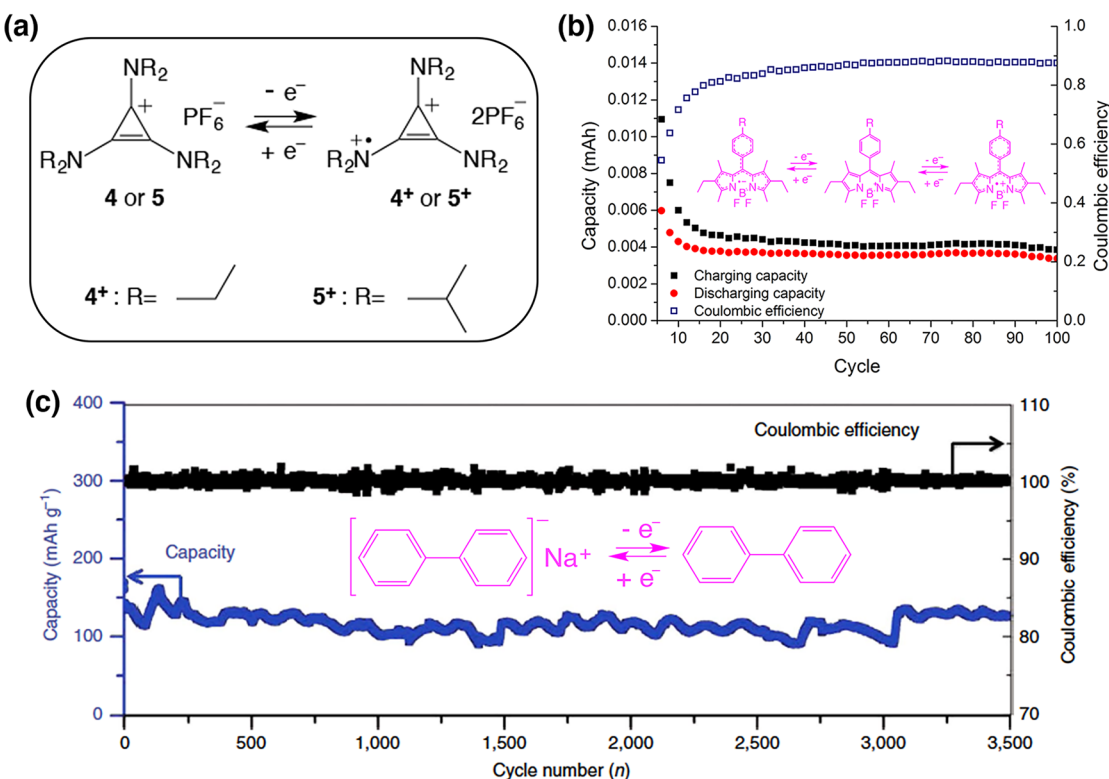


Figure 10. (a) Electrochemistry of cyclopropenium derivatives;<sup>119</sup> (b) cycling performance of a nonaqueous all-BODIPY RFB (Adapted with permission from the American Chemical Society);<sup>120</sup> (c) cycling performance of a nonflow Na-biphenyl/polysulfides battery at  $1100 \text{ mAg}^{-1}$  (Adapted with permission from Springer Nature).<sup>121</sup>

with solvent and electrolyte, leading to improved flow cell cyclability at battery-relevant ROM concentrations (0.5 M) higher than those of other nonaqueous all-organic RFBs. Odom et al. demonstrated high-potential phenothiazine-based catholyte materials for nonaqueous RFB applications.<sup>115,116</sup> Interestingly, the charged radical cation salts were successfully prepared via chemical oxidation and isolated as pure materials, which allowed straightforward testing of chemical stability in a symmetric RFB cell using a 1:1 mixture of phenothiazine and its salt. Constant cycling capacity for 100 cycles without detectable loss was achieved, indicating the excellent stability of phenothiazine species.

In aqueous RFBs, the redox potentials of heterocyclic aromatics should fall within the voltage window of water. As previously mentioned, **N**-alkylated viologen derivatives were demonstrated as promising anolyte ROMs coupled with TEMPO<sup>52,107</sup> and Fc species<sup>49,79</sup> because of its high solubility ( $>3 \text{ M}$ ), low potential ( $-0.45 \text{ V}$  vs NHE), and high stability. With Fc catholytes, the RFBs delivered exceptionally stable cycling for at least 500 cycles with  $>90\%$  capacity retention (Figure 5c). Aziz et al.<sup>117</sup> and Meng et al.<sup>118</sup> independently developed bio-inspired flavin cofactors with alloxazine-based redox core structures as  $2\text{e}^-$  anolyte materials. Structural engineering to remove

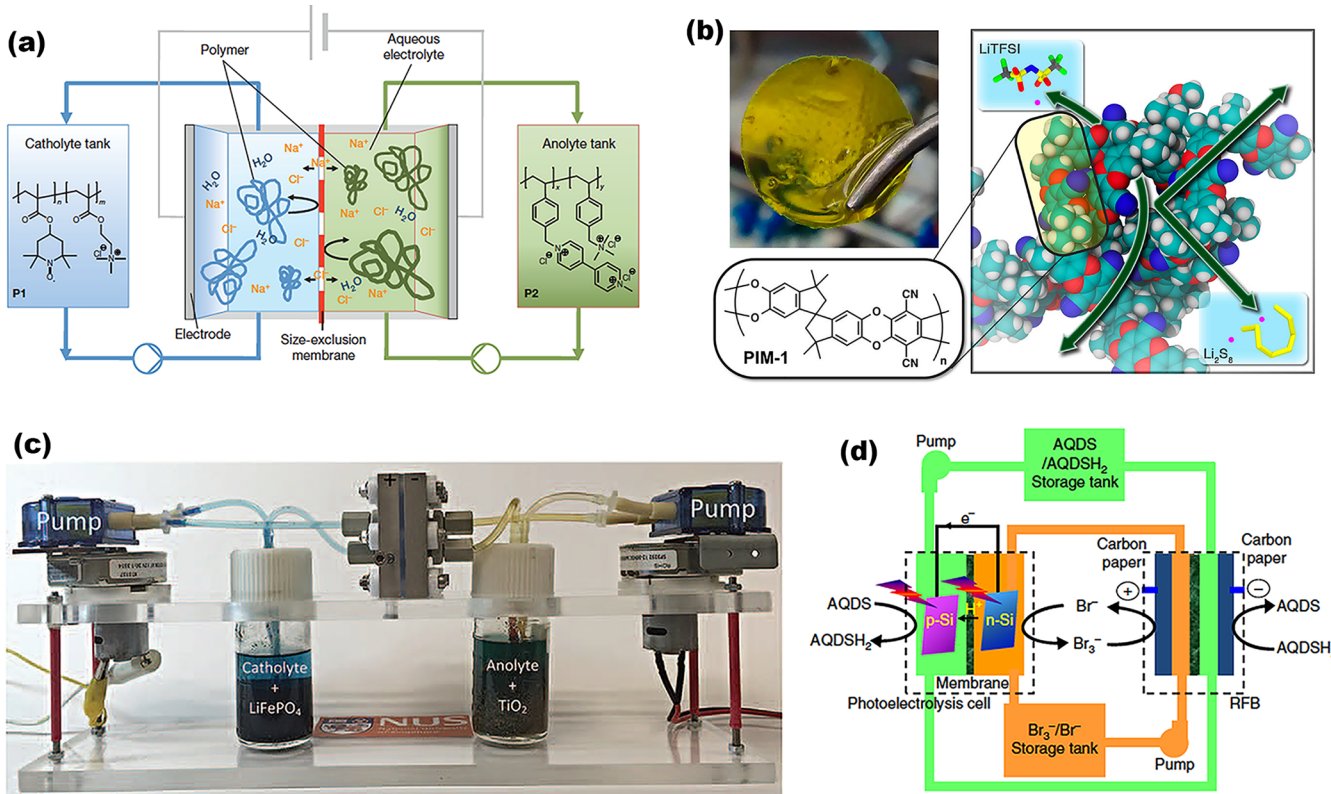


Figure 11. (a) Schematic representation of an aqueous RAP-based RFB using poly-TEMPO catholyte and polyviologen anolyte (Reproduced with permission from Springer Nature);<sup>134</sup> (b) photo, composition, and pore size modeling of a PIM membrane for blocking polysulfide crossover (Reproduced with permission from the American Chemical Society);<sup>138</sup> (c) setup of a redox targeting RFB (Reproduced with permission from American Association for the Advancement of Science);<sup>141</sup> (d) schematic representation of a solar rechargeable RFB (Reproduced with permission from Springer Nature).<sup>142</sup>

the N-substituent was found to be important to obtain chemically stable derivatives in alkaline electrolytes. When coupled with the ferrocyanide/ferricyanide pair, the alloxazine-based RFBs produced high cycling stability with 91% capacity retention for 400 cycles (Figure 9b).

These impressive battery performances demonstrate the great potential of heterocyclic aromatics toward fostering practically relevant organic RFB systems. Further research efforts could focus on the invention of new ROMs of this type with competitive solubility and stability, as well as high compatibility with acidic supporting electrolytes to improve power density. In addition, despite the high cycling stability, the ROM crossover across the membrane throughout a long-term, decade-scale cycling remains a concern because this will cause irreversible capacity loss and thus determine the service life of organic RFBs.

**Other ROM Molecules.** Besides the above-mentioned ROMs, other lesser-investigated structural motifs have been reported for RFB applications. Sanford et al. developed a series of aromatic cyclopropenium salts as cyclable, high-potential catholyte materials for nonaqueous RFBs (Figure 10a).<sup>119</sup> The promising derivatives had redox potentials of  $\geq 0.8$  V vs Fc/Fc<sup>+</sup> when oxidized to form radical dications and underwent stable BE cell cycling at nearly 100% SOC for 200 cycles with <3% capacity fading. Schubert et al. demonstrated a nonaqueous symmetric RFB based on boron-dipyrrromethene (BODIPY)-containing redox-active copolymers.<sup>120</sup> BODIPY undergoes ambipolar electrochemical reactions and thus was demonstrated in an all-BODIPY RFB albeit the rate performance and cell efficiencies

were rather limited (Figure 10b). Hu et al. developed a low-potential anolyte material consisting of a highly soluble Na-biphenyl compound (Figure 10c) that was coupled with polysulfide catholyte.<sup>121</sup> With a sodium  $\beta$ -alumina separator, this nonaqueous battery demonstrated a high energy density of 201 Wh L<sup>-1</sup> and a long cycling stability for 3500 cycles without capacity fading, indicating the high promise of the Na-biphenyl species. Yang et al. demonstrated a conductive polymer-based nonaqueous symmetric RFB using polythiophene microparticle dispersions as both anodic and cathodic couples.<sup>122</sup> The RFB exhibited a cell voltage of 2.5 V and decent cycling stability for 30 cycles but suffered from poor rate performance primarily due to limited ion diffusion rates in the particulate active materials. Fu et al. demonstrated highly soluble organotrisulfide-based catholyte materials that are capable of 4 e<sup>-</sup> transfer.<sup>123</sup> A high energy density of 158 Wh L<sup>-1</sup> was achieved when a diphenyl trisulfide catholyte was coupled with Li anode.

**Other Organic RFB Materials and Designs.** Crossover Mitigation. Crossover of redox materials is one of the major reasons for capacity fading in both aqueous and nonaqueous RFBs, even though the crossover is low in certain systems. The determining factor is the membrane properties including the composition, pore size, stability, and mechanical strength. For aqueous RFBs, ion exchange membranes are widely used due to the low crossover, while porous separators are also used in certain systems such as VRBs, iron/chromium, and iron/vanadium.<sup>124–127</sup> However, the membrane issue is more challenging for nonaqueous RFBs due to the limited choices of suitable membranes, although a number of membranes have

been evaluated. Ion exchange membranes including Nafion generally suffer from low materials selectivity and ionic conductivity.<sup>128–130</sup> Ceramic LISICON-type separators have superior selectivity but encounter poor ionic conductivity, mechanical properties, and scalability. Porous separators such as Daramic, Celgard, and Tonen have high conductivity but are limited by low materials selectivity. Flexible membranes combining high selectivity and conductivity are urgently needed to make nonaqueous RFBs deliver good cyclability at battery-relevant conditions and achieve practical breakthroughs.

The capacity decays in VRBs and symmetric RFBs can possibly be restored through electrolyte remixing or pressure regulation.<sup>131,132</sup> However, for RFBs based on two different redox compounds, such crossover is irreversible, leading to unrecoverable capacity loss and inferior cell efficiencies. To overcome this limitation, mixed-reactant electrolytes have been used in certain systems, such as iron/chromium,<sup>133</sup> iron/vanadium,<sup>13,14</sup> and several organic systems,<sup>88–90</sup> to reduce the concentration gradients across the membrane and improve the cyclability. However, this usually sacrifices half of the materials concentration, increases the electrolyte viscosity, poses more strict stability requirements with no degradation reactions in the whole voltage range, yet still fails to completely eliminate the crossover of the charged species especially in the case of porous separators.

On the basis of the size exclusion rule, two alternative strategies have been explored to address the crossover issue in organic RFBs. First, bulky redox-active polymers (RAPs), with organic pendants such as viologen and TEMPO attached to the backbone, were developed for RFB applications (Figure 11a).<sup>134–137</sup> The significantly large molecular size increased the crossover barrier for RAPs, leading to improved cycling stability and enabling the use of cost-effective porous separators. Despite these advantages, the effective molarities of redox-active motifs in RAPs are typically lower compared to the monomers due to the solvophobic polymer backbone, and the increase of electrolyte viscosity is not nontrivial. These disadvantages will potentially compromise the energy density and cycling efficiency of RAP-based RFBs.

Second, membranes made of polymers of intrinsic micro-porosity (PIM), with greatly shrunk pore sizes (<2 nm) as compared to conventional porous separators (>20 nm), were developed for RFB applications (Figure 11b).<sup>138–140</sup> Such small pores yielded more than 500-fold improvement in the membrane selectivity while the small thickness still maintained good conductivity, making PIM membranes a promising alternative membrane option for organic RFBs. In the future, the compositions of these PIM membranes need to be intelligently engineered to tune the pore size, chemical stability, swelling, and mechanical strength.

**Redox Targeting RFBs.** As shown in Figure 11c, the redox targeting concept is a synergy between RFBs and LIBs, capitalizing on flowable solutions of redox shuttles mediating reactions of static LIB electrode materials.<sup>141,143</sup> The LIB materials stored in external tanks with no carbon additives aim for high energy density, while the RFB that typically uses dilute mediator solutions offers design flexibility and high power density. Two mediator molecules are used with redox potentials straddling that of the LIB material. Electrochemical conversions of redox mediators in the RFB and chemical intercalation/deintercalation of the LIB materials in the tanks occur step by step.

Rational selection of mediator molecules is pivotal for enabling redox targeting RFBs to deliver high cycling efficiency

and stability. Metallocenes are the most studied mediator molecules because of their desirable redox potentials and high chemical stability. Wang et al. demonstrated the redox targeting half cells of LiFePO<sub>4</sub> with Fc and 1,1'-dibromoferrocene (FcBr<sub>2</sub>) mediators<sup>144</sup> and of anatase TiO<sub>2</sub> with cobaltocene (CoCp<sub>2</sub>) and decamethylcobaltocene (CoCp<sub>2</sub>\*<sub>2</sub>) mediators.<sup>145</sup> A full cell of these two delivered a volumetric energy density of 238 Wh L<sup>-1</sup> and decent cyclability for ~50 cycles.<sup>141</sup> More recent examples include ethyl viologen and iodide mediators for Prussian blue<sup>146</sup> and a 2 e<sup>-</sup> 2,3,5,6-tetramethyl-*p*-phenylenediamine mediator for LiFeO<sub>4</sub>.<sup>147</sup> In addition, the redox targeting approach has been extended to develop a Li–sulfur RFB with totally insulating sulfur cathodes by using decamethylnickelocene and decamethylchromocene mediators<sup>148</sup> and a Li–O<sub>2</sub> RFB with mitigated passivation and pore clogging of the cathode by using ethyl viologen and iodide mediators.<sup>149</sup>

**Solar Rechargeable RFBs.** Solar rechargeable RFBs are hybrid battery devices integrating photoelectrochemical cells (PECs) and RFB cells. Upon solar illumination of the photoelectrodes, the generated holes and photoelectrons convert the catholyte and anolyte redox couples in the RFB, respectively. As such, direct storage of the energy generated from solar is achieved; the discharge is like that in normal RFBs to deliver electricity. As a key requirement, the redox couple at the photoelectrode side entails a suitable redox potential matched with the band positions of the photoelectrode. The traditional design of solar rechargeable RFBs was based on dye-sensitized solar cells, and the most studied couple was iodide/triiodide paired with different RFB couples.<sup>150–155</sup> Recently, organic couples have also been evaluated as the photoelectrode-side couple inspired by recent material advances in organic RFBs. Jin et al.<sup>156</sup> and Li et al.<sup>142</sup> independently demonstrated tailored anthraquinones for use in solar rechargeable RFBs because of their versatile properties, with dual-silicon PECs overcoming the intrinsic limitations of traditionally used dye-sensitized photoelectrodes (Figure 11d). These systems achieved high photocharging currents up to 10 mA cm<sup>-2</sup> and solar-to-electricity conversion efficiency up to 3.2%.

**Computational Studies.** In developing competitive organic RFBs, one of the major challenges is the search for promising ROMs with favored combination of properties such as redox potential, solubility, and stability. Considering the practically infinite library of organic candidates, the trial-and-error experimentation strategy will be low-efficiency and time-consuming. Alternatively, the theoretical computations have demonstrated great efficacy in expediting the development of promising ROMs. The acquired theoretical understandings of the quantitative structure–property relationships will in turn guide rational design and prototyping of optimal ROMs. Prior computational studies of the stability and interactions of organic species in RAPs can shed light on the current research of ROMs.<sup>70,157,158</sup>

Theoretical calculations such as DFT-based frameworks can derive intrinsic properties of ROMs that are relevant for RFB applications. The redox potentials of ROMs were computed from the solution-phase Gibbs free energy change ( $\Delta G_{\text{red}}$  or  $\Delta G_{\text{ox}}$ ) for adding or losing an electron, while the solubility was predicted from the solvation free energy ( $\Delta G_{\text{solv}}$ ).<sup>159,160</sup> The calculation results have led to identification of ROMs and RFB systems with practically pertinent solubilities and cell voltages. Furthermore, computational chemistry can play a role in predicting and mitigating materials degradation. Typically, the stability of ROMs was predicted by computing the Gibbs free

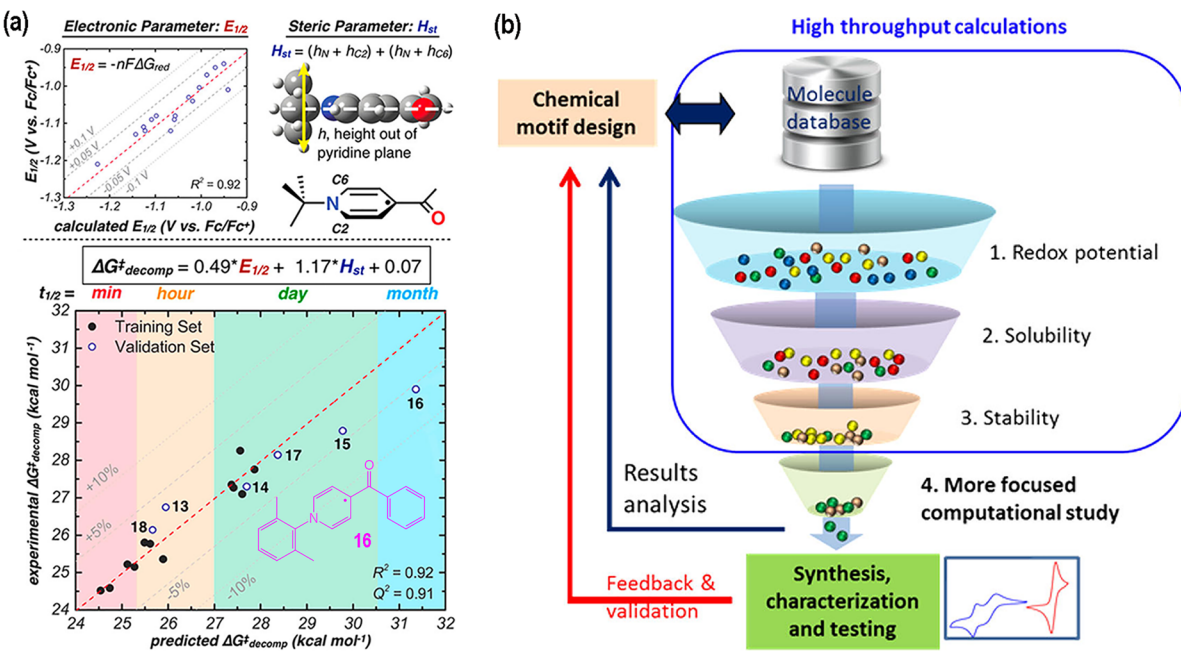


**Figure 12.** (a) Quantitative physical organic model incorporating both electronic ( $E_{1/2}$ ) and steric ( $H_{st}$ ) descriptors to develop persistent radical analogue 16 (Reproduced with permission from the American Chemical Society);<sup>114</sup> (b) schematic of high-throughput computational down-selection pipeline for ROM-based RFBs with successive property tiers (Reproduced with permission from the American Chemical Society).<sup>162</sup>

energies and activation enthalpies for likely side reactions to gain insights into the thermodynamic and kinetic driving forces for these decomposition pathways.<sup>161</sup> Because many ROMs involve radical ions upon electrochemical charging, computations of steric and configurational parameters could also give insights of radical stability, especially when a large number of substituents are possible. Interestingly, Sanford et al. presented a quantitative physical organic model that incorporated comprehensive electronic and steric parameters, combined with experimental approaches, to predict and obtain the most persistent *N*-alkylpyridinium radical 16 (Figure 12a) out of its 18 delicately designed derivatives (among them, analogue 17 is shown in Figure 9a).<sup>114</sup>

On the basis of the statements above, computational high-throughput screening strategies have emerged for accelerated discovery of propitious ROMs for RFB applications. An Electrolyte genome quantum chemical calculation infrastructure was developed establishing a database of large amounts of ROM molecules and electrolyte systems.<sup>163</sup> A hierarchical computational pipeline was presented for down-selection of a pool of ROM candidates from >10 000 molecules through successive property evaluations of the redox potential, solubility, and stability (Figure 12b).<sup>162</sup> Such computational tools in combination with experimental investigations can offer cost-effective avenues for design and optimization of suitable ROM candidates with a greatly shortened time frame.

**Summary and Future Outlook.** We have summarized the state-of-the-art of the development of organic RFB materials and systems. Significant progress has been achieved in the past decade to greatly advance organic RFB technologies. Adopting organic electrochemistry greatly expands the materials selection range and redox mechanism diversity for RFB development. ROMs have offered broad space for enabling exceeding performance merits in terms of higher cell voltages, better solubilities, faster electrochemical kinetics, and exceptional cyclability for

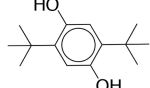
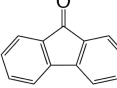
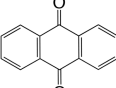
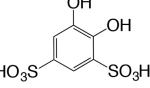
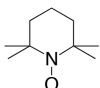
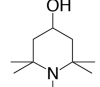
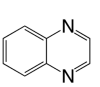
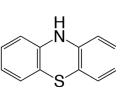
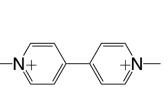
Adopting organic electrochemistry greatly expands the materials selection range and redox mechanism diversity for RFB development. ROMs have offered broad space for enabling exceeding performance merits in terms of higher cell voltages, better solubilities, faster electrochemical kinetics, and exceptional cyclability for RFBs compared to their inorganic counterparts.

RFBs compared to their inorganic counterparts. In addition, the cost-effectiveness is an important advantage of ROMs, as shown in Table 2 listing the bulk prices of a majority of the above-mentioned ROMs or their precursors.

Despite these advantages, it is still too early for organic RFBs to gain market penetration. The following technical and financial challenges need to be addressed before organic RFBs become practically viable and gain industrial attention.

**Energy Density.** The solubility of ROMs directly determines the deliverable energy density of organic RFBs. So far, only a few organic compounds exhibit exceeding solubilities of >3 M compared to their major competitor VRB.<sup>49,90,102,107</sup> Incorporation of polar functional groups to the core structures has been proven effective in increasing the molecular dipole moment and improving the ROM solubility. Moreover, most reported systems operated at ROM concentrations well below their solubility limits, with one of the major reasons being the lower solubility of charged species. More in-depth studies should include the solubilities of all of the redox species involved in cell reactions, as well as the thermal stability of electrolytes.<sup>12</sup> Finally, ROMs that allow multiple electron

**Table 2.** Bulk Prices of Prominent ROMs or Their Precursors in \$ kg<sup>-1</sup> at a Scale of 25 kg from Alibaba.com, unless Otherwise Indicated<sup>164,a</sup>

ROMs						
ferrocene	1 <sup>49</sup>	1~5	2	4.74 <sup>51</sup>	5~10 <sup>99</sup>	5~7
Prices	1 <sup>49</sup>	1~5	2	4.74 <sup>51</sup>	5~10 <sup>99</sup>	5~7
ROMs						
4-hydroxy-TEMPO	7 <sup>52</sup>	1~20	1~2	1~2	1 <sup>52</sup>	10~12
Prices	7 <sup>52</sup>	1~20	1~2	1~2	1 <sup>52</sup>	10~12

<sup>a</sup>The price of V<sub>2</sub>O<sub>5</sub> is listed as a reference.

transfers should be investigated as a promising pathway to achieve high energy density.

**Stability.** The stability of ROMs determines the cycle life of organic RFBs. Especially, electrochemistry of organic compounds typically involves relatively reactive radicals in charged species. Capacity fading has been observed in a number of organic RFBs with chemical instability as one major reason.<sup>52,93,106</sup> Fundamental understandings of degradation mechanisms can effectively guide further structural designs and electrolyte optimizations for stability improvement.<sup>88,95,165</sup> Both ex situ and in situ chemical characterizations are essentially important tools to unveil the pathways of parasitic side reactions of ROMs, which should be incorporated in studying ROM-based RFBs.

**Efficiency.** The efficiencies of organic RFBs are affected by a variety of factors, including side reactions, electrolyte conductivity, membrane resistivity, self-discharge, electrochemical kinetics, electrodes, and cell design. Systematic material and system optimizations are needed for a given organic RFB chemistry to boost efficiency. Electrolyte engineering is often needed for organic RFBs to increase ionic conductivity, cell voltage, and redox material solubility and compatibility.<sup>88</sup> This is especially true for nonaqueous RFBs that generally have high electrolyte viscosities. Moreover, RFB cell designs including electrode dimension and flow field (flow-through, serpentine, or interdigitated) play an important role in reducing cell polarization and improving rate performance.<sup>116,166</sup> Finally, the electrode is a critical yet underexplored area for organic RFBs. The morphologies (felts, papers, or cloths) and surface functionalities (including electrocatalysts) on carbon electrode materials have significant effects on interfacial charge transfer kinetics.<sup>39,167</sup>

**Membrane.** Ideally, crossover-free membranes could enable organic RFBs to deliver infinitely long cycling for stable ROMs. In reality, unbalanced ROM crossover typically causes continuous capacity loss in RFBs even at low ROM concentrations. Strategies such as mixed-reactant electrolytes, PIM membranes, and bulky RAPs are effective to some extent to improve cyclability but fail to completely eliminate ROM crossover. In addition, undesirable material–membrane interactions could cause ROMs trapped in membranes for organic RFBs, leading to reduced conductivity and materials loss. Membranes that combine high ionic conductivity and material-to-charge carrier

selectivity are still urgently needed for organic RFBs to enable high efficiency and cycling stability.

**Cost.** Inexpensive ROMs are favored to enable cost-effective organic RFB systems. The material cost level of <\$200 per kWh has been claimed in a few organic RFBs.<sup>49,51,52</sup> The ROMs should be either commercially available with industrial-scale productions or easily manufacturable from cheap precursors via scalable synthetic methods. The estimation of system and operational costs could rely on more comprehensive cost models.<sup>168</sup>

## ■ AUTHOR INFORMATION

### Corresponding Author

\*E-mail: Xiaoliang.Wei@pnnl.gov. Phone: 01-509-371-6493.

### ORCID

Xiaoliang Wei: 0000-0002-7692-2357

Jun Liu: 0000-0001-8663-7771

Wei Wang: 0000-0002-5453-4695

### Notes

The authors declare no competing financial interest.

### Biographies

**Xiaoliang Wei** obtained his Ph.D. in chemistry from Brown University and currently is a staff scientist at Pacific Northwest National Laboratory. His research expertise includes energy conversion and storage, self-assembled materials, and organic/polymer chemistry. He has published >40 peer-reviewed journal articles and earned the Ronald L. Brodzinski Early Career Exceptional Achievement Award.

**Wenxiao Pan** is an assistant professor at the University of Wisconsin—Madison. She received her Ph.D. in applied mathematics at Brown University in 2010. Her research focuses on multiscale modeling and computing with application in energy storage systems, soft materials, and complex fluids.

**Wentao Duan** received his Ph.D. degree in 2015 from Pennsylvania State University and is currently a postdoctoral researcher at Pacific Northwest National Laboratory. His research focuses on energy conversion and storage.

**Aaron Hollas** received his B.S. in Chemistry from Texas A&M University and his Ph.D. from the University of California—Irvine. He is currently a postdoctoral research associate at Pacific Northwest

National Laboratory where he works on developing new redox-active organic molecules for aqueous redox flow batteries.

**Zheng Yang** is a postdoctoral researcher at Pacific Northwest National Laboratory. His research interests include development and application of the science and technology of organic redox species and systems for aqueous and nonaqueous redox flow batteries.

**Bin Li** received his Ph.D. in materials science & engineering from Tsinghua University in 2010. He is now a staff scientist at Pacific Northwest National Laboratory. His research is focused on redox flow batteries, multivalent ion batteries, and fuel cells in the field of energy storage and conversion.

**Zimin Nie** is a senior scientist at Pacific Northwest National Laboratory. She has extensive expertise in electrochemical energy conversion and storage and materials synthesis and characterizations. She has published more than 100 journal papers and has received an R&D 100 Award and a Federal Laboratory Consortium Award for Technology Transfer.

**Jun Liu** obtained his Ph.D. in materials science and engineering from the University of Washington and currently is a Battelle Fellow at Pacific Northwest National Laboratory and the Director of the U.S. DOE's Battery500 Consortium. His research areas include nanostructured materials and applications for energy, catalysis, environments, and health.

**David Reed** is a senior scientist and team lead in the Electrochemical Materials and Systems Group at Pacific Northwest National Laboratory. His research includes stationary energy storage, high-temperature electrochemistry, fuel cells, electroceramics, and building efficiency.

**Wei Wang** is a senior scientist at Pacific Northwest National Laboratory, where he is currently leading the research and development of stationary energy storage technologies. Dr. Wang received his Ph.D. in materials science and engineering from Carnegie Mellon University in 2009.

**Vincent Sprenkle** is the project manager for the U.S. DOE Office of Electricity Energy Storage Program and the technical group manager for the Electrochemical Materials and Systems Group at Pacific Northwest National Laboratory. His research includes energy storage, fuel cells, ceramics, and oxygen production.

## ACKNOWLEDGMENTS

This research was financially supported by the Joint Center for Energy Storage Research (JCESR), an Energy Innovation Hub funded by the U.S. Department of Energy (DOE), Office of Science, Basic Energy Sciences, and by the Energy Storage Program of U.S. DOE's Office of Electricity Delivery and Energy Reliability (OE) under Contract No. 57558. PNNL is a multiprogram national laboratory operated by Battelle for DOE under Contract DE-AC05-76RL01830.

## REFERENCES

- (1) *International Energy Outlook 2016, With Projections To 2040*; U.S. Energy Information Administration (EIA), DOE/EIA-0484; 2016.
- (2) Eber, K.; Corbus, D. *Hawaii Solar Integration Study: Executive Summary*; U.S. National Renewable Energy Laboratory (NREL), NREL/TP-5500-57215; 2013.
- (3) Larcher, D.; Tarascon, J. M. Towards greener and more sustainable batteries for electrical energy storage. *Nat. Chem.* **2015**, *7* (1), 19–29.
- (4) Dunn, B.; Kamath, H.; Tarascon, J. M. Electrical Energy Storage for the Grid: A Battery of Choices. *Science* **2011**, *334*, 928–935.

(5) Yang, Z. G.; Zhang, J.; Kintner-Meyer, M. C. W.; Lu, X.; Choi, D.; Lemmon, J. P.; Liu, J. *Electrochemical Energy Storage for Green Grid*. *Chem. Rev.* **2011**, *111* (5), 3577–3613.

(6) Badwal, S. P. S.; Giddey, S. S.; Munnings, C.; Bhatt, A. I.; Hollenkamp, A. F. Emerging electrochemical energy conversion and storage technologies. *Front. Chem.* **2014**, DOI: 10.3389/fchem.2014.00079.

(7) US Department of Energy, Office of Electricity Delivery & Energy Reliability. *Global Energy Storage Database*. <https://www.energystorageexchange.org/> (Accessed February 17, 2017).

(8) *Global battery energy storage market for smart grid 2016–2020*. SKU: IRTNTR9659; Technavio, 2016.

(9) Nykvist, B.; Nilsson, M. Rapidly falling costs of battery packs for electric vehicles. *Nat. Clim. Change* **2015**, *5* (4), 329–332.

(10) Choi, J.; Aurbach, D. Promise and reality of post-lithium-ion batteries with high energy densities. *Nat. Rev. Mater.* **2016**, *1*, 16013.

(11) Skyllas-Kazacos, M.; Rychcik, M.; Robins, R. G.; Fane, A. G.; Green, M. A. New All-Vanadium Redox Flow Cell. *J. Electrochem. Soc.* **1986**, *133* (5), 1057–1058.

(12) Li, L.; Kim, S.; Wang, W.; Vijayakumar, M.; Nie, Z.; Chen, B.; Zhang, J.; Xia, G.; Hu, J.; Graff, G.; Liu, J.; Yang, Z. G. A Stable Vanadium Redox-Flow Battery with High Energy Density for Large-Scale Energy Storage. *Adv. Energy Mater.* **2011**, *1* (3), 394–400.

(13) Wang, W.; Nie, Z.; Chen, B.; Chen, F.; Luo, Q.; Wei, X.; Xia, G.; Skyllas-Kazacos, M.; Li, L.; Yang, Z. G. A New Fe/V Redox Flow Battery Using a Sulfuric/Chloric Mixed-Acid Supporting Electrolyte. *Adv. Energy Mater.* **2012**, *2* (4), 487–493.

(14) Wang, W.; Kim, S.; Chen, B.; Nie, Z.; Zhang, J.; Xia, G.; Li, L.; Yang, Z. G. A new redox flow battery using Fe/V redox couples in chloride supporting electrolyte. *Energy Environ. Sci.* **2011**, *4* (10), 4068–4073.

(15) Thaller, L. H. *Recent advances in redox flow cell storage systems*; NASA TM-79186, DOE/NASA/1002-79/4; 1979.

(16) Remick, R. J.; Ang, P. G. P. Electrically rechargeable anionically active reduction-oxidation electrical storage-supply system. U.S. Patent 4485154, 1984.

(17) Lim, H.; Lackner, A. M.; Knechtli, R. C. Zinc-Bromine Secondary Battery. *J. Electrochem. Soc.* **1977**, *124* (8), 1154–1157.

(18) Li, B.; Nie, Z.; Vijayakumar, M.; Li, G.; Liu, J.; Sprenkle, V.; Wang, W. Ambipolar zinc-polyiodide electrolyte for a high-energy density aqueous redox flow battery. *Nat. Commun.* **2015**, *6*, 6303.

(19) Leung, P. K.; Ponce-de-Leon, C.; Low, C. T. J.; Shah, A. A.; Walsh, F. C. Characterization of a zinc-cerium flow battery. *J. Power Sources* **2011**, *196* (11), 5174–5185.

(20) Verde, M. G.; Carroll, K. J.; Wang, Z.; Sathrum, A.; Meng, Y. S. Achieving high efficiency and cyclability in inexpensive soluble lead flow batteries. *Energy Environ. Sci.* **2013**, *6* (5), 1573–1581.

(21) Braff, W. A.; Bazant, M. Z.; Buie, C. R. Membrane-less hydrogen bromine flow battery. *Nat. Commun.* **2013**, *4*, 2346.

(22) Wei, X.; Xia, G.; Kirby, B.; Thomesen, E.; Li, B.; Nie, Z.; Graff, G. G.; Liu, J.; Sprenkle, V.; Wang, W. An Aqueous Redox Flow Battery Based on Neutral Alkali Metal Ferri/ferrocyanide and Polysulfide Electrolytes. *J. Electrochem. Soc.* **2016**, *163* (1), A5150–A5153.

(23) Hawthorne, K. L.; Wainright, J. S.; Savinell, R. F. Studies of Iron-Ligand Complexes for an All-Iron Flow Battery Application. *J. Electrochem. Soc.* **2014**, *161* (10), A1662–A1671.

(24) Gong, K.; Xu, F.; Grunewald, J. B.; Ma, X.; Zhao, Y.; Gu, S.; Yan, Y. All-Soluble All-Iron Aqueous Redox-Flow Battery. *ACS Energy Lett.* **2016**, *1* (1), 89–93.

(25) Skyllas-Kazacos, M.; Chakrabarti, M. H.; Hajimolana, S. A.; Mjalli, F. S.; Saleem, M. Progress in Flow Battery Research and Development. *J. Electrochem. Soc.* **2011**, *158* (8), R55–R79.

(26) Weber, A. Z.; Mench, M. M.; Meyers, J. P.; Ross, P. N.; Gostick, J. T.; Liu, Q. Redox flow batteries: a review. *J. Appl. Electrochem.* **2011**, *41* (10), 1137–1164.

(27) Leung, P.; Li, X.; Ponce de Leon, C.; Berlouis, L.; Low, C. T. J.; Walsh, F. C. Progress in redox flow batteries, remaining challenges and their applications in energy storage. *RSC Adv.* **2012**, *2* (27), 10125–10156.

- (28) Soloveichik, G. L. Flow Batteries: Current Status and Trends. *Chem. Rev.* **2015**, *115* (20), 11533–11558.
- (29) Perry, M. L.; Weber, A. Z. Advanced Redox-Flow Batteries: A Perspective. *J. Electrochem. Soc.* **2016**, *163* (1), A5064–A5067.
- (30) Park, M.; Ryu, J.; Wang, W.; Cho, J. Material design and engineering of next-generation flow-battery technologies. *Nat. Rev. Mater.* **2016**, *2* (1), 16080.
- (31) Li, B.; Liu, J. Progress and directions in low-cost redox-flow batteries for large-scale energy storage. *Natl. Sci. Rev.* **2017**, *4* (1), 91–105.
- (32) Wang, W.; Luo, Q.; Li, B.; Wei, X.; Li, L.; Yang, Z. G. Recent Progress in Redox Flow Battery Research and Development. *Adv. Funct. Mater.* **2013**, *23* (8), 970–986.
- (33) Darling, R. M.; Gallagher, K. G.; Kowalski, J. A.; Ha, S.; Brushett, F. R. Pathways to low-cost electrochemical energy storage: a comparison of aqueous and nonaqueous flow batteries. *Energy Environ. Sci.* **2014**, *7* (11), 3459–3477.
- (34) Ding, C.; Zhang, H.; Li, X.; Liu, T.; Xing, F. Vanadium Flow Battery for Energy Storage: Prospects and Challenges. *J. Phys. Chem. Lett.* **2013**, *4* (8), 1281–1294.
- (35) Crawford, A.; Viswanathan, V.; Stephenson, D.; Wang, W.; Thomsen, E.; Reed, D.; Li, B.; Baldacci, P.; Kintner-Meyer, M.; Sprenkle, V. Comparative analysis for various redox flow batteries chemistries using a cost performance model. *J. Power Sources* **2015**, *293*, 388–399.
- (36) *Chemicoool*. <http://www.chemicoool.com/>. (Accessed August 21, 2017).
- (37) Roe, S.; Menictas, C.; Skyllas-Kazacos, M. A High Energy Density Vanadium Redox Flow Battery with 3 M Vanadium Electrolyte. *J. Electrochem. Soc.* **2016**, *163* (1), A5023–A5028.
- (38) Li, L. Unique Advantages of Chloride-Containing all Vanadium Redox Flow Battery. 2017 Fall MRS Meeting, Boston, MA; 2017.
- (39) Li, B.; Gu, M.; Nie, Z.; Shao, Y.; Luo, Q.; Wei, X.; Li, X.; Xiao, J.; Wang, C.; Sprenkle, V.; Wang, W. Bismuth Nanoparticle Decorating Graphite Felt as a High-Performance Electrode for an All-Vanadium Redox Flow Battery. *Nano Lett.* **2013**, *13* (3), 1330–1335.
- (40) Zeng, Y.; Zhao, T.; An, L.; Zhou, X.; Wei, L. A comparative study of all-vanadium and iron-chromium redox flow batteries for large-scale energy storage. *J. Power Sources* **2015**, *300*, 438–443.
- (41) Zhao, P.; Zhang, H.; Zhou, H.; Yi, B. Nickel foam and carbon felt applications for sodium poly sulfide/bromine redox flow battery electrodes. *Electrochim. Acta* **2005**, *51* (6), 1091–1098.
- (42) Wang, C.; Lai, Q.; Xu, P.; Zheng, D.; Li, X.; Zhang, H. Cage-Like Porous Carbon with Superhigh Activity and Br<sub>2</sub>-Complex-Entrapping Capability for Bromine-Based Flow Batteries. *Adv. Mater.* **2017**, *29* (22), 1605815.
- (43) Li, B.; Liu, J.; Nie, Z.; Wang, W.; Reed, D.; Liu, J.; McGrail, P.; Sprenkle, V. Metal Organic Frameworks as Highly Active Electrocatalysts for High-Energy Density, Aqueous Zinc-Polyiodide Redox Flow Batteries. *Nano Lett.* **2016**, *16* (7), 4335–4340.
- (44) Oury, A.; Kirchev, A.; Bultel, Y. Cycling of soluble lead flow cells comprising a honeycomb-shaped positive electrode. *J. Power Sources* **2014**, *264*, 22–29.
- (45) Lin, G.; Chong, P. Y.; Yarlagadda, V.; Nguyen, T. V.; Wycisk, R. J.; Pintauro, P. N.; Bates, M.; Mukerjee, S.; Tucker, M. C.; Weber, A. Z. Advanced Hydrogen-Bromine Flow Batteries with Improved Efficiency, Durability and Cost. *J. Electrochem. Soc.* **2016**, *163* (1), A5049–A5056.
- (46) Zhao, Y.; Byon, H. High-Performance Lithium-Iodine Flow Battery. *Adv. Energy Mater.* **2013**, *3* (12), 1630–1635.
- (47) Chen, H.; Lu, Y. A High-Energy-Density Multiple Redox Semi-Solid-Liquid Flow Battery. *Adv. Energy Mater.* **2016**, *6* (8), 1502183.
- (48) Duduta, M.; Ho, B.; Wood, V. C.; Limthongkul, P.; Brunini, V. E.; Carter, W. C.; Chiang, Y. M. Semi-Solid Lithium Rechargeable Flow Battery. *Adv. Energy Mater.* **2011**, *1* (4), 511–516.
- (49) Hu, B.; DeBruler, C.; Rhodes, Z.; Liu, T. L. Long-Cycling Aqueous Organic Redox Flow Battery (AORFB) toward Sustainable and Safe Energy Storage. *J. Am. Chem. Soc.* **2017**, *139* (3), 1207–1214.
- (50) Zhang, J.; Yang, Z.; Shkrob, I. A.; Assary, R. S.; Tung, S. o.; Silcox, B.; Duan, W.; Zhang, J.; Su, C. C.; Hu, B.; Pan, B.; Liao, C.; Zhang, Z.; Wang, W.; Curtiss, L. A.; Thompson, L. T.; Wei, X.; Zhang, L. Annulated Dialkoxybenzenes as Catholyte Materials for Non-aqueous Redox Flow Batteries: Achieving High Chemical Stability through Bicyclic Substitution. *Adv. Energy Mater.* **2017**, *7*, 1701272.
- (51) Huskinson, B.; Marshak, M. P.; Suh, C.; Er, S.; Gerhardt, M. R.; Galvin, C. J.; Chen, X.; Aspuru-Guzik, A.; Gordon, R. G.; Aziz, M. J. A metal-free organic-inorganic aqueous flow battery. *Nature* **2014**, *505* (7482), 195–198.
- (52) Liu, T.; Wei, X.; Nie, Z.; Sprenkle, V.; Wang, W. A Total Organic Aqueous Redox Flow Battery Employing a Low Cost and Sustainable Methyl Viologen Anolyte and 4-HO-TEMPO Catholyte. *Adv. Energy Mater.* **2016**, *6* (3), 1501449.
- (53) Shin, S.; Yun, S.; Moon, S. A review of current developments in non-aqueous redox flow batteries: characterization of their membranes for design perspective. *RSC Adv.* **2013**, *3* (24), 9095–9116.
- (54) Gong, K.; Fang, Q.; Gu, S.; Li, S.; Yan, Y. Nonaqueous redox-flow batteries: organic solvents, supporting electrolytes, and redox pairs. *Energy Environ. Sci.* **2015**, *8* (12), 3515–3530.
- (55) Zhao, Y.; Ding, Y.; Li, Y.; Peng, L.; Byon, H.; Goodenough, J. B.; Yu, G. A chemistry and material perspective on lithium redox flow batteries towards high-density electrical energy storage. *Chem. Soc. Rev.* **2015**, *44* (22), 7968–7996.
- (56) Fan, F. Y.; Woodford, W. H.; Li, Z.; Baram, N.; Smith, K. C.; Helal, A.; McKinley, G. H.; Carter, W. C.; Chiang, Y. M. Polysulfide Flow Batteries Enabled by Percolating Nanoscale Conductor Networks. *Nano Lett.* **2014**, *14* (4), 2210–2218.
- (57) Lu, Y.; Goodenough, J. B. Rechargeable alkali-ion cathode-flow battery. *J. Mater. Chem.* **2011**, *21* (27), 10113–10117.
- (58) Wang, Y.; Wang, Y.; Zhou, H. A Li-Liquid Cathode Battery Based on a Hybrid Electrolyte. *ChemSusChem* **2011**, *4* (8), 1087–1090.
- (59) Yang, Y.; Zheng, G.; Cui, Y. A membrane-free lithium/polysulfide semi-liquid battery for large-scale energy storage. *Energy Environ. Sci.* **2013**, *6* (5), 1552–1558.
- (60) Pan, H.; Wei, X.; Henderson, W. A.; Shao, Y.; Chen, J.; Bhattacharya, P.; Xiao, J.; Liu, J. On the Way Toward Understanding Solution Chemistry of Lithium Polysulfides for High Energy Li-S Redox Flow Batteries. *Adv. Energy Mater.* **2015**, *5* (16), 1500113.
- (61) Wei, X.; Cosimescu, L.; Xu, W.; Hu, J.; Vijayakumar, M.; Feng, J.; Hu, M. Y.; Deng, X.; Xiao, J.; Liu, J.; Sprenkle, V.; Wang, W. Towards High-Performance Nonaqueous Redox Flow Electrolyte Via Ionic Modification of Active Species. *Adv. Energy Mater.* **2015**, *5* (1), 1400678.
- (62) Zhao, Y.; Ding, Y.; Song, J.; Li, G.; Dong, G.; Goodenough, J. B.; Yu, G. Sustainable Electrical Energy Storage through the Ferrocene/Ferrocenium Redox Reaction in Aprotic Electrolyte. *Angew. Chem., Int. Ed.* **2014**, *53* (41), 11036–11040.
- (63) Liu, Q.; Sleightholme, A. E. S.; Shinkle, A. A.; Li, Y.; Thompson, L. T. Non-aqueous vanadium acetylacetone electrolyte for redox flow batteries. *Electrochim. Commun.* **2009**, *11* (12), 2312–2315.
- (64) Pratt, H. D.; Hudak, N. S.; Fang, X.; Anderson, T. M. A polyoxometalate flow battery. *J. Power Sources* **2013**, *236*, 259–264.
- (65) Pratt, H. D., III; Rose, A. J.; Staiger, C. L.; Ingersoll, D.; Anderson, T. M. Synthesis and characterization of ionic liquids containing copper, manganese, or zinc coordination cations. *Dalton Trans.* **2011**, *40* (43), 11396–11401.
- (66) Cappillino, P. J.; Pratt, H. D.; Hudak, N. S.; Tomson, N. C.; Anderson, T. M.; Anstey, M. R. Application of Redox Non-Innocent Ligands to Non-Aqueous Flow Battery Electrolytes. *Adv. Energy Mater.* **2014**, *4* (1), 1300566.
- (67) Sevov, C. S.; Fisher, S. L.; Thompson, L. T.; Sanford, M. S. Mechanism-Based Development of a Low-Potential, Soluble, and Cyclable Multielectron Anolyte for Nonaqueous Redox Flow Batteries. *J. Am. Chem. Soc.* **2016**, *138* (47), 15378–15384.
- (68) Liang, Y.; Tao, Z.; Chen, J. Organic Electrode Materials for Rechargeable Lithium Batteries. *Adv. Energy Mater.* **2012**, *2* (7), 742–769.

- (69) Song, Z.; Zhou, H. Towards sustainable and versatile energy storage devices: an overview of organic electrode materials. *Energy Environ. Sci.* **2013**, *6* (8), 2280–2301.
- (70) Schon, T. B.; McAllister, B. T.; Li, P.; Seferos, D. S. The rise of organic electrode materials for energy storage (vol 45, pg 6345, 2016). *Chem. Soc. Rev.* **2016**, *45* (22), 6405–6406.
- (71) Noack, J.; Roznyatovskaya, N.; Herr, T.; Fischer, P. The Chemistry of Redox-Flow Batteries. *Angew. Chem., Int. Ed.* **2015**, *54* (34), 9776–9809.
- (72) Winsberg, J.; Hagemann, T.; Janoschka, T.; Hager, M. D.; Schubert, U. S. Redox-Flow Batteries: From Metals to Organic Redox-Active Materials. *Angew. Chem., Int. Ed.* **2017**, *56*, 686–711.
- (73) Leung, P.; Shah, A. A.; Sanz, L.; Flox, C.; Morante, J. R.; Xu, Q.; Mohamed, M. R.; Ponce de Leon, C.; Walsh, F. C. Recent developments in organic redox flow batteries: A Critical Review. *J. Power Sources* **2017**, *360*, 243–283.
- (74) Vanýsek, P. Electrochemical Series. In *CRC Handbook of Chemistry and Physics*, 94th ed. (Internet Version); Haynes, W. M., Ed.; CRC Press/Taylor and Francis: Boca Raton, FL, 2014.
- (75) Ding, Y.; Zhao, Y.; Yu, G. A membrane-free ferrocene-based high-rate semiliquid battery. *Nano Lett.* **2015**, *15* (6), 4108–4113.
- (76) Cosimescu, L.; Wei, X.; Vijayakumar, M.; Xu, W.; Helm, M. L.; Burton, S. D.; Sorensen, C. M.; Liu, J.; Sprenkle, V.; Wang, W. Anion-Tunable Properties and Electrochemical Performance of Functionalized Ferrocene Compounds. *Sci. Rep.* **2015**, *14117*.
- (77) Hwang, B.; Park, M.; Kim, K. Ferrocene and Cobaltocene Derivatives for Non-Aqueous Redox Flow Batteries. *ChemSusChem* **2015**, *8* (2), 310–314.
- (78) Cong, G.; Zhou, Y.; Li, Z.; Lu, Y. A Highly Concentrated Catholyte Enabled by a Low-Melting-Point Ferrocene Derivative. *ACS Energy Lett.* **2017**, *2* (4), 869–875.
- (79) Beh, E. S.; De Porcellinis, D.; Gracia, R. L.; Xia, K.; Gordon, R. G.; Aziz, M. J. A Neutral pH Aqueous Organic-Organometallic Redox Flow Battery with Extremely High Capacity Retention. *ACS Energy Lett.* **2017**, *2* (3), 639–644.
- (80) Han, K.; Rajput, N. N.; Vijayakumar, M.; Wei, X.; Wang, W.; Hu, J.; Persson, K. A.; Mueller, K. T. Preferential Solvation of an Asymmetric Redox Molecule. *J. Phys. Chem. C* **2016**, *120* (49), 27834–27839.
- (81) Deng, X.; Hu, M.; Wei, X.; Wang, W.; Mueller, K. T.; Chen, Z.; Hu, J. Nuclear magnetic resonance studies of the solvation structures of a high-performance nonaqueous redox flow electrolyte. *J. Power Sources* **2016**, *308*, 172–179.
- (82) Han, K.; Rajput, N. N.; Wei, X.; Wang, W.; Hu, J.; Persson, K. A.; Mueller, K. T. Diffusional motion of redox centers in carbonate electrolytes. *J. Chem. Phys.* **2014**, *141* (10), 104509.
- (83) Ding, Y.; Zhao, Y.; Li, Y.; Goodenough, J. B.; Yu, G. A high-performance all-metallocene-based, non-aqueous redox flow battery. *Energy Environ. Sci.* **2017**, *10*, 491–497.
- (84) Peljo, P.; Bichon, M.; Girault, H. H. Ion transfer battery: storing energy by transferring ions across liquid-liquid interfaces. *Chem. Commun.* **2016**, *52* (63), 9761–9764.
- (85) Brushett, F. R.; Vaughney, J. T.; Jansen, A. N. An All-Organic Non-aqueous Lithium-Ion Redox Flow Battery. *Adv. Energy Mater.* **2012**, *2* (11), 1390–1396.
- (86) Zhang, L.; Zhang, Z.; Redfern, P. C.; Curtiss, L. A.; Amine, K. Molecular engineering towards safer lithium-ion batteries: a highly stable and compatible redox shuttle for overcharge protection. *Energy Environ. Sci.* **2012**, *5* (8), 8204–8207.
- (87) Huang, J.; Cheng, L.; Assary, R. S.; Wang, P.; Xue, Z.; Burrell, A. K.; Curtiss, L. A.; Zhang, L. Liquid Catholyte Molecules for Nonaqueous Redox Flow Batteries. *Adv. Energy Mater.* **2015**, *5* (6), 1401782.
- (88) Wei, X.; Xu, W.; Huang, J.; Zhang, L.; Walter, E.; Lawrence, C.; Vijayakumar, M.; Henderson, W. A.; Liu, T.; Cosimescu, L.; Li, B.; Sprenkle, V.; Wang, W. Radical Compatibility with Nonaqueous Electrolytes and Its Impact on an All-Organic Redox Flow Battery. *Angew. Chem., Int. Ed.* **2015**, *54* (30), 8684–8687.
- (89) Wei, X.; Duan, W.; Huang, J.; Zhang, L.; Li, B.; Reed, D.; Xu, W.; Sprenkle, V.; Wang, W. A High-Current, Stable Nonaqueous Organic Redox Flow Battery. *ACS Energy Lett.* **2016**, *1* (4), 705–711.
- (90) Duan, W.; Huang, J.; Kowalski, J. A.; Shkrob, I. A.; Vijayakumar, M.; Walter, E.; Pan, B.; Yang, Z.; Milshtein, J. D.; Li, B.; Liao, C.; Zhang, Z.; Wang, W.; Liu, J.; Moore, J. S.; Brushett, F. R.; Zhang, L.; Wei, X. "Wine-Dark Sea" in an Organic Flow Battery: Storing Negative Charge in 2,1,3-Benzothiadiazole Radicals Leads to Improved Cyclability. *ACS Energy Lett.* **2017**, *2* (5), 1156–1161.
- (91) Huang, J.; Su, L.; Kowalski, J. A.; Barton, J. L.; Ferrandon, M.; Burrell, A. K.; Brushett, F. R.; Zhang, L. A subtractive approach to molecular engineering of dimethoxybenzene-based redox materials for non-aqueous flow batteries. *J. Mater. Chem. A* **2015**, *3* (29), 14971–14976.
- (92) Huang, J.; Pan, B.; Duan, W.; Wei, X.; Assary, R. S.; Su, L.; Brushett, F. R.; Cheng, L.; Liao, C.; Ferrandon, M. S.; Wang, W.; Zhang, Z.; Burrell, A. K.; Curtiss, L. A.; Shkrob, I. A.; Moore, J. S.; Zhang, L. The lightest organic radical cation for charge storage in redox flow batteries. *Sci. Rep.* **2016**, *32102*.
- (93) Hooper-Burkhardt, L.; Krishnamoorthy, S.; Yang, B.; Murali, A.; Nirmalchandar, A.; Prakash, G. K. S.; Narayanan, S. R. A New Michael-Reaction-Resistant Benzoquinone for Aqueous Organic Redox Flow Batteries. *J. Electrochem. Soc.* **2017**, *164* (4), A600–A607.
- (94) Wang, W.; Xu, W.; Cosimescu, L.; Choi, D.; Li, L.; Yang, Z. G. Anthraquinone with tailored structure for a nonaqueous metal-organic redox flow battery. *Chem. Commun.* **2012**, *48* (53), 6669–6671.
- (95) Carney, T. J.; Collins, S. J.; Moore, J. S.; Brushett, F. R. Concentration-Dependent Dimerization of Anthraquinone Disulfonic Acid and Its Impact on Charge Storage. *Chem. Mater.* **2017**, *29* (11), 4801–4810.
- (96) Chen, Q.; Gerhardt, M. R.; Hartle, L.; Aziz, M. J. A Quinone-Bromide Flow Battery with 1 W/cm<sup>2</sup> Power Density. *J. Electrochem. Soc.* **2016**, *163* (1), A5010–A5013.
- (97) Gerhardt, M. R.; Tong, L.; Gomez-Bombarelli, R.; Chen, Q.; Marshak, M. P.; Galvin, C. J.; Aspuru-Guzik, A.; Gordon, R. G.; Aziz, M. J. Anthraquinone Derivatives in Aqueous Flow Batteries. *Adv. Energy Mater.* **2017**, *7* (8), 1601488.
- (98) Lin, K.; Chen, Q.; Gerhardt, M. R.; Tong, L.; Kim, S. B.; Eisenach, L.; Valle, A. W.; Hardee, D.; Gordon, R. G.; Aziz, M. J.; Marshak, M. P. Alkaline quinone flow battery. *Science* **2015**, *349* (6255), 1529–1532.
- (99) Yang, B.; Hooper-Burkhardt, L.; Wang, F.; Surya Prakash, G. K.; Narayanan, S. R. An Inexpensive Aqueous Flow Battery for Large-Scale Electrical Energy Storage Based on Water-Soluble Organic Redox Couples. *J. Electrochem. Soc.* **2014**, *161* (9), A1371–A1380.
- (100) Yang, B.; Hooper-Burkhardt, L.; Krishnamoorthy, S.; Murali, A.; Prakash, G. K. S.; Narayanan, S. R. High-Performance Aqueous Organic Flow Battery with Quinone-Based Redox Couples at Both Electrodes. *J. Electrochem. Soc.* **2016**, *163* (7), A1442–A1449.
- (101) Lalevee, J.; Allonas, X.; Jacques, P. Electronic distribution and solvatochromism investigation of a model radical (2,2,6,6-tetramethylpiperidine N-oxyl: tempo) through TD-DFT calculations including PCM solvation. *J. Mol. Struct.: THEOCHEM* **2006**, *767* (1–3), 143–147.
- (102) Wei, X.; Xu, W.; Vijayakumar, M.; Cosimescu, L.; Liu, T.; Sprenkle, V.; Wang, W. TEMPO-Based Catholyte for High-Energy Density Nonaqueous Redox Flow Batteries. *Adv. Mater.* **2014**, *26* (45), 7649–7653.
- (103) Li, Z.; Li, S.; Liu, S.; Huang, K.; Fang, D.; Wang, F.; Peng, S. Electrochemical Properties of an All-Organic Redox Flow Battery Using 2,2,6,6-Tetramethyl-1-Piperidinyloxy and N-Methylphthalimide. *Electrochim. Solid-State Lett.* **2011**, *14* (12), A171–A173.
- (104) Park, S.; Shim, J.; Yang, J.; Shin, K.; Jin, C.; Lee, B.; Lee, Y.; Jeon, J. Electrochemical properties of a non-aqueous redox battery with all-organic redox couples. *Electrochim. Commun.* **2015**, *59*, 68–71.
- (105) Takechi, K.; Kato, Y.; Hase, Y. A Highly Concentrated Catholyte Based on a Solvate Ionic Liquid for Rechargeable Flow Batteries. *Adv. Mater.* **2015**, *27* (15), 2501–2506.

- (106) Duan, W.; Vemuri, R. S.; Milshtein, J. D.; Laramie, S.; Dmello, R. D.; Huang, J.; Zhang, L.; Hu, D.; Vijayakumar, M.; Wang, W.; Liu, J.; Darling, R. M.; Thompson, L.; Smith, K.; Moore, J. S.; Brushett, F. R.; Wei, X. A symmetric organic-based nonaqueous redox flow battery and its state of charge diagnostics by FTIR. *J. Mater. Chem. A* **2016**, *4* (15), 5448–5456.
- (107) Janoschka, T.; Martin, N.; Hager, M. D.; Schubert, U. S. An Aqueous Redox-Flow Battery with High Capacity and Power: The TEMPTMA/MV System. *Angew. Chem., Int. Ed.* **2016**, *55* (46), 14427–14430.
- (108) Winsberg, J.; Stolze, C.; Schwenke, A.; Muench, S.; Hager, M. D.; Schubert, U. S. Aqueous 2,2,6,6-Tetramethylpiperidine-N-oxyl Catholytes for a High-Capacity and High Current Density Oxygen-Insensitive Hybrid-Flow Battery. *ACS Energy Lett.* **2017**, *2* (2), 411–416.
- (109) Duan, W.; Vemuri, R. S.; Hu, D.; Yang, Z.; Wei, X. A Protocol for Electrochemical Evaluations and State of Charge Diagnostics of a Symmetric Organic Redox Flow Battery. *J. Visualized Exp.* **2017**, No. 120, e55171.
- (110) Carretero-Gonzalez, J.; Castillo-Martinez, E.; Armand, M. Highly water-soluble three-redox state organic dyes as bifunctional analytes. *Energy Environ. Sci.* **2016**, *9* (11), 3521–3530.
- (111) Potash, R. A.; McKone, J. R.; Conte, S.; Abruna, H. D. On the Benefits of a Symmetric Redox Flow Battery. *J. Electrochem. Soc.* **2016**, *163* (3), A338–A344.
- (112) Milshtein, J. D.; Su, L.; Liou, C.; Badel, A. F.; Brushett, F. R. Voltammetry study of quinoxaline in aqueous electrolytes. *Electrochim. Acta* **2015**, *180*, 695–704.
- (113) Sevov, C. S.; Brooner, R. E. M.; Chenard, E.; Assary, R. S.; Moore, J. S.; Rodriguez-Lopez, J.; Sanford, M. S. Evolutionary Design of Low Molecular Weight Organic Anolyte Materials for Applications in Nonaqueous Redox Flow Batteries. *J. Am. Chem. Soc.* **2015**, *137* (45), 14465–14472.
- (114) Sevov, C. S.; Hickey, D. P.; Cook, M. E.; Robinson, S. G.; Barnett, S.; Minteer, S. D.; Sigman, M. S.; Sanford, M. S. Physical Organic Approach to Persistent, Cyclable, Low-Potential Electrolytes for Flow Battery Applications. *J. Am. Chem. Soc.* **2017**, *139* (8), 2924–2927.
- (115) Kaur, A. P.; Holubowitch, N. E.; Ergun, S.; Elliott, C. F.; Odom, S. A. A Highly Soluble Organic Catholyte for Non-Aqueous Redox Flow Batteries. *Energy Technol.* **2015**, *3* (5), 476–480.
- (116) Milshtein, J. D.; Kaur, A. P.; Casselman, M. D.; Kowalski, J. A.; Modekrutti, S.; Zhang, P. L.; Harsha Attanayake, N.; Elliott, C. F.; Parkin, S. R.; Risko, C.; Brushett, F. R.; Odom, S. A. High current density, long duration cycling of soluble organic active species for non-aqueous redox flow batteries. *Energy Environ. Sci.* **2016**, *9* (11), 3531–3543.
- (117) Lin, K.; Gomez-Bombarelli, R.; Beh, E. S.; Tong, L.; Chen, Q.; Valle, A.; Aspuru-Guzik, A.; Aziz, M. J.; Gordon, R. G. A redox-flow battery with an alloxazine-based organic electrolyte. *Nat. Energy* **2016**, *1*, 16102.
- (118) Orita, A.; Verde, M. G.; Sakai, M.; Meng, Y. S. A biomimetic redox flow battery based on flavin mononucleotide. *Nat. Commun.* **2016**, *7*, 13230.
- (119) Sevov, C. S.; Samaroo, S. K.; Sanford, M. S. Cyclopropenium Salts as Cyclable, High-Potential Catholytes in Nonaqueous Media. *Adv. Energy Mater.* **2017**, *7* (5), 1602027.
- (120) Winsberg, J.; Hagemann, T.; Muench, S.; Fribe, C.; Haupler, B.; Janoschka, T.; Morgenstern, S.; Hager, M. D.; Schubert, U. S. Poly(boron-dipyromethene)-A Redox-Active Polymer Class for Polymer Redox-Flow Batteries. *Chem. Mater.* **2016**, *28* (10), 3401–3405.
- (121) Yu, J.; Hu, Y.; Pan, F.; Zhang, Z.; Wang, Q.; Li, H.; Huang, X.; Chen, L. A class of liquid anode for rechargeable batteries with ultralong cycle life. *Nat. Commun.* **2017**, *8*, 14629.
- (122) Oh, S.; Lee, C.; Chun, D.; Jeon, J.; Shim, J.; Shin, K.; Yang, J. A metal-free and all-organic redox flow battery with polythiophene as the electroactive species. *J. Mater. Chem. A* **2014**, *2* (47), 19994–19998.
- (123) Wu, M.; Bhargav, A.; Cui, Y.; Siegel, A.; Agarwal, M.; Ma, Y.; Fu, Y. Highly Reversible Diphenyl Trisulfide Catholyte for Rechargeable Lithium Batteries. *ACS Energy Lett.* **2016**, *1* (6), 1221–1226.
- (124) Zhang, H.; Zhang, H.; Li, X.; Mai, Z.; Zhang, J. Nanofiltration (NF) membranes: the next generation separators for all vanadium redox flow batteries (VRBs)? *Energy Environ. Sci.* **2011**, *4* (5), 1676–1679.
- (125) Wei, X.; Nie, Z.; Luo, Q.; Li, B.; Chen, B.; Simmons, K.; Sprenkle, V.; Wang, W. Nanoporous Polytetrafl uoroethylene/Silica Composite Separator as a High-Performance All-Vanadium Redox Flow Battery Membrane. *Adv. Energy Mater.* **2013**, *3* (9), 1215–1220.
- (126) Wei, X.; Nie, Z.; Luo, Q.; Li, B.; Sprenkle, V.; Wang, W. Polyvinyl Chloride/Silica Nanoporous Composite Separator for All-Vanadium Redox Flow Battery Applications. *J. Electrochem. Soc.* **2013**, *160* (8), A1215–A1218.
- (127) Wei, X.; Li, L.; Luo, Q.; Nie, Z.; Wang, W.; Li, B.; Xia, G.; Miller, E.; Chambers, J.; Yang, Z. G. Microporous separators for Fe/V redox flow batteries. *J. Power Sources* **2012**, *218*, 39–45.
- (128) Su, L.; Darling, R. M.; Gallagher, K. G.; Xie, W.; Thelen, J. L.; Badel, A. F.; Barton, J. L.; Cheng, K. J.; Balsara, N. P.; Moore, J. S.; Brushett, F. R. An Investigation of the Ionic Conductivity and Species Crossover of Lithiated Nafion 117 in Nonaqueous Electrolytes. *J. Electrochem. Soc.* **2016**, *163* (1), A5253–A5262.
- (129) Small, L. J.; Pratt, H. D.; Fujimoto, C. H.; Anderson, T. M. Diels Alder Polyphenylene Anion Exchange Membrane for Nonaqueous Redox Flow Batteries. *J. Electrochem. Soc.* **2016**, *163* (1), A5106–A5111.
- (130) Hudak, N. S.; Small, L. J.; Pratt, H. D.; Anderson, T. M. Through-Plane Conductivities of Membranes for Nonaqueous Redox Flow Batteries. *J. Electrochem. Soc.* **2015**, *162* (10), A2188–A2194.
- (131) Luo, Q.; Li, L.; Wang, W.; Nie, Z.; Wei, X.; Li, B.; Chen, B.; Yang, Z. G.; Sprenkle, V. Capacity Decay and Remediation of Nafion-based All-Vanadium Redox Flow Batteries. *ChemSusChem* **2013**, *6* (2), 268–274.
- (132) Li, B.; Luo, Q.; Wei, X.; Nie, Z.; Thomsen, E.; Chen, B.; Sprenkle, V.; Wang, W. Capacity Decay Mechanism of Microporous Separator-Based All-Vanadium Redox Flow Batteries and its Recovery. *ChemSusChem* **2014**, *7* (2), 577–584.
- (133) Lopezatalaya, M.; Codina, G.; Perez, J. R.; Vazquez, J. L.; Aldaz, A. Optimization Studies on a Fe/Cr Redox Flow Battery. *J. Power Sources* **1992**, *39* (2), 147–154.
- (134) Janoschka, T.; Martin, N.; Martin, U.; Fribe, C.; Morgenstern, S.; Hiller, H.; Hager, M. D.; Schubert, U. S. An aqueous, polymer-based redox-flow battery using non-corrosive, safe, and low-cost materials. *Nature* **2015**, *527* (7576), 78–81.
- (135) Winsberg, J.; Janoschka, T.; Morgenstern, S.; Hagemann, T.; Muench, S.; Hauffmann, G.; Gohy, J. F.; Hager, M. D.; Schubert, U. S. Poly(TEMPO)/Zinc Hybrid-Flow Battery: A Novel, "Green," High Voltage, and Safe Energy Storage System. *Adv. Mater.* **2016**, *28* (11), 2238–2243.
- (136) Nagarjuna, G.; Hui, J.; Cheng, K. J.; Lichtenstein, T.; Shen, M.; Moore, J. S.; Rodriguez-Lopez, J. Impact of Redox-Active Polymer Molecular Weight on the Electrochemical Properties and Transport Across Porous Separators in Nonaqueous Solvents. *J. Am. Chem. Soc.* **2014**, *136* (46), 16309–16316.
- (137) Montoto, E. C.; Nagarjuna, G.; Hui, J.; Burgess, M.; Sekerak, N. M.; Hernandez-Burgos, K.; Wei, T. S.; Kneer, M.; Grolman, J.; Cheng, K. J.; Lewis, J. A.; Moore, J. S.; Rodriguez-Lopez, J. Redox Active Colloids as Discrete Energy Storage Carriers. *J. Am. Chem. Soc.* **2016**, *138* (40), 13230–13237.
- (138) Li, C.; Ward, A. L.; Doris, S. E.; Pascal, T. A.; Prendergast, D.; Helms, B. A. Polysulfide-Blocking Microporous Polymer Membrane Tailored for Hybrid Li-Sulfur Flow Batteries. *Nano Lett.* **2015**, *15* (9), 5724–5729.
- (139) Chae, I.; Luo, T.; Moon, G.; Oieglo, W.; Kang, Y.; Wessling, M. Ultra-High Proton/Vanadium Selectivity for Hydrophobic Polymer Membranes with Intrinsic Nanopores for Redox Flow Battery. *Adv. Energy Mater.* **2016**, *6* (16), 1600517.

- (140) Doris, S. E.; Ward, A. L.; Baskin, A.; Frischmann, P. D.; Gavvalapalli, N.; Chenard, E.; Sevov, C. S.; Prendergast, D.; Moore, J. S.; Helms, B. A. Macromolecular Design Strategies for Preventing Active-Material Crossover in Non-Aqueous All-Organic Redox-Flow Batteries. *Angew. Chem., Int. Ed.* **2017**, *56* (6), 1595–1599.
- (141) Jia, C.; Pan, F.; Zhu, Y.; Huang, Q.; Lu, L.; Wang, Q. High-energy density nonaqueous all redox flow lithium battery enabled with a polymeric membrane. *Sci. Adv.* **2015**, *1* (20), e1500886.
- (142) Liao, S.; Zong, X.; Seger, B.; Pedersen, T.; Yao, T.; Ding, C.; Shi, J.; Chen, J.; Li, C. Integrating a dual-silicon photoelectrochemical cell into a redox flow battery for unassisted photocharging. *Nat. Commun.* **2016**, *7*, 11474.
- (143) Huang, Q.; Yang, J.; Ng, C. B.; Jia, C.; Wang, Q. A redox flow lithium battery based on the redox targeting reactions between LiFePO<sub>4</sub> and iodide. *Energy Environ. Sci.* **2016**, *9* (3), 917–921.
- (144) Huang, Q.; Li, H.; Gratzel, M.; Wang, Q. Reversible chemical delithiation/lithiation of LiFePO<sub>4</sub>: towards a redox flow lithium-ion battery. *Phys. Chem. Chem. Phys.* **2013**, *15* (6), 1793–1797.
- (145) Pan, F.; Yang, J.; Huang, Q.; Wang, X.; Huang, H.; Wang, Q. Redox Targeting of Anatase TiO<sub>2</sub> for Redox Flow Lithium-Ion Batteries. *Adv. Energy Mater.* **2014**, *4* (15), 1400567.
- (146) Fan, L.; Jia, C.; Zhu, Y.; Wang, Q. Redox Targeting of Prussian Blue: Toward Low-Cost and High Energy Density Redox Flow Battery and Solar Rechargeable Battery. *ACS Energy Lett.* **2017**, *2* (3), 615–621.
- (147) Zhu, Y.; Du, Y.; Jia, C.; Zhou, M.; Fan, L.; Wang, X.; Wang, Q. Unleashing the Power and Energy of LiFePO<sub>4</sub>-Based Redox Flow Lithium Battery with a Bifunctional Redox Mediator. *J. Am. Chem. Soc.* **2017**, *139* (18), 6286–6289.
- (148) Li, J.; Yang, L.; Yang, S.; Lee, J. The Application of Redox Targeting Principles to the Design of Rechargeable Li-S Flow Batteries. *Adv. Energy Mater.* **2015**, *5* (24), 1501808.
- (149) Zhu, Y.; Jia, C.; Yang, J.; Pan, F.; Huang, Q.; Wang, Q. Dual redox catalysts for oxygen reduction and evolution reactions: towards a redox flow Li-O<sub>2</sub> battery. *Chem. Commun.* **2015**, *51* (46), 9451–9454.
- (150) Liu, P.; Cao, Y.; Li, G.; Gao, X.; Ai, X.; Yang, H. A Solar Rechargeable Flow Battery Based on Photoregeneration of Two Soluble Redox Couples. *ChemSusChem* **2013**, *6* (5), 802–806.
- (151) Yan, N.; Li, G.; Gao, X. Solar rechargeable redox flow battery based on Li<sub>2</sub>WO<sub>4</sub>/LiI couples in dual-phase electrolytes. *J. Mater. Chem. A* **2013**, *1* (24), 7012–7015.
- (152) Yu, M.; McCulloch, W. D.; Beauchamp, D. R.; Huang, Z.; Ren, X.; Wu, Y. Aqueous Lithium-Iodine Solar Flow Battery for the Simultaneous Conversion and Storage of Solar Energy. *J. Am. Chem. Soc.* **2015**, *137* (26), 8332–8335.
- (153) Mahmoudzadeh, M. A.; Usgaocar, A. R.; Giorgio, J.; Officer, D. L.; Wallace, G. G.; Madden, J. D. W. A high energy density solar rechargeable redox battery. *J. Mater. Chem. A* **2016**, *4* (9), 3446–3452.
- (154) Nikiforidis, G.; Tajima, K.; Byon, H. High Energy Efficiency and Stability for Photoassisted Aqueous Lithium-Iodine Redox Batteries. *ACS Energy Lett.* **2016**, *1* (4), 806–813.
- (155) McCulloch, W. D.; Yu, M.; Wu, Y. pH-Tuning a Solar Redox Flow Battery for Integrated Energy Conversion and Storage. *ACS Energy Lett.* **2016**, *1* (3), 578–582.
- (156) Li, W.; Fu, H.; Li, L.; Caban-Acevedo, M.; He, J.; Jin, S. Integrated Photoelectrochemical Solar Energy Conversion and Organic Redox Flow Battery Devices. *Angew. Chem., Int. Ed.* **2016**, *55* (42), 13104–13108.
- (157) Jain, A.; Shin, Y.; Persson, K. A. Computational predictions of energy materials using density functional theory. *Nat. Rev. Mater.* **2016**, *1*, 15004.
- (158) Kanal, I. Y.; Owens, S. G.; Bechtel, J. S.; Hutchison, G. R. Efficient Computational Screening of Organic Polymer Photovoltaics. *J. Phys. Chem. Lett.* **2013**, *4* (10), 1613–1623.
- (159) Er, S.; Suh, C.; Marshak, M. P.; Aspuru-Guzik, A. Computational design of molecules for an all-quinone redox flow battery. *Chem. Sci.* **2015**, *6* (2), 885–893.
- (160) Pineda Flores, S. D.; Martin-Noble, G. C.; Phillips, R. L.; Schrier, J. Bio-Inspired Electroactive Organic Molecules for Aqueous Redox Flow Batteries. 1. Thiophenoquinones. *J. Phys. Chem. C* **2015**, *119* (38), 21800–21809.
- (161) Assary, R. S.; Zhang, L.; Huang, J.; Curtiss, L. A. Molecular Level Understanding of the Factors Affecting the Stability of Dimethoxy Benzene Catholyte Candidates from First-Principles Investigations. *J. Phys. Chem. C* **2016**, *120* (27), 14531–14538.
- (162) Cheng, L.; Assary, R. S.; Qu, X.; Jain, A.; Ong, S. P.; Rajput, N. N.; Persson, K.; Curtiss, L. A. Accelerating Electrolyte Discovery for Energy Storage with High-Throughput Screening. *J. Phys. Chem. Lett.* **2015**, *6* (2), 283–291.
- (163) Qu, X.; Jain, A.; Rajput, N. N.; Cheng, L.; Zhang, Y.; Ong, S. P.; Brafman, M.; Maginn, E.; Curtiss, L. A.; Persson, K. A. The Electrolyte Genome project: A big data approach in battery materials discovery. *Comput. Mater. Sci.* **2015**, *103*, 56–67.
- (164) Obtained as the lowest prices from [Alibaba.com](http://Alibaba.com) (Accessed August 18, 2018).
- (165) Carino, E. V.; Staszak-Jirkovsky, J.; Assary, R. S.; Curtiss, L. A.; Markovic, N. M.; Brushett, F. R. Tuning the Stability of Organic Active Materials for Nonaqueous Redox Flow Batteries via Reversible, Electrochemically Mediated Li<sup>+</sup> Coordination. *Chem. Mater.* **2016**, *28*, 2529–2539.
- (166) Li, X. Modeling and simulation study of a metal free organic-inorganic aqueous flow battery with flow through electrode. *Electrochim. Acta* **2015**, *170*, 98–109.
- (167) Zhou, X.; Zhao, T.; Zeng, Y.; An, L.; Wei, L. A highly permeable and enhanced surface area carbon-cloth electrode for vanadium redox flow batteries. *J. Power Sources* **2016**, *329*, 247–254.
- (168) Viswanathan, V.; Crawford, A.; Stephenson, D.; Kim, S.; Wang, W.; Li, B.; Coffey, G.; Thomsen, E.; Graff, G.; Balducci, P.; Kintner-Meyer, M.; Sprengle, V. Cost and performance model for redox flow batteries. *J. Power Sources* **2014**, *247*, 1040–1051.